

---

# Co-Adaptation of Algorithmic and Implementational Innovations in Inference-based Deep Reinforcement Learning

---

**Hiroki Furuta**  
The University of Tokyo  
furuta@weblab.t.u-tokyo.ac.jp

**Tadashi Kozuno**  
University of Alberta

**Tatsuya Matsushima**  
The University of Tokyo

**Yutaka Matsuo**  
The University of Tokyo

**Shixiang Shane Gu**  
Google Research

## Abstract

Recently many algorithms were devised for reinforcement learning (RL) with function approximation. While they have clear algorithmic distinctions, they also have many implementation differences that are algorithm-independent and sometimes under-emphasized. Such mixing of algorithmic novelty and implementation craftsmanship makes rigorous analyses of the sources of performance improvements across algorithms difficult. In this work, we focus on a series of off-policy inference-based actor-critic algorithms – MPO, AWR, and SAC – to decouple their algorithmic innovations and implementation decisions. We present unified derivations through a single control-as-inference objective, where we can categorize each algorithm as based on either Expectation-Maximization (EM) or direct Kullback-Leibler (KL) divergence minimization and treat the rest of specifications as implementation details. We performed extensive ablation studies, and identified substantial performance drops whenever implementation details are *mismatched* for algorithmic choices. These results show which implementation or code details are co-adapted and co-evolved with algorithms, and which are transferable across algorithms: as examples, we identified that tanh Gaussian policy and network sizes are highly adapted to algorithmic types, while layer normalization and ELU are critical for MPO’s performances but also transfer to noticeable gains in SAC. We hope our work can inspire future work to further demystify sources of performance improvements across multiple algorithms and allow researchers to build on one another’s both algorithmic and implementational innovations.<sup>1</sup>

## 1 Introduction

Deep reinforcement learning (RL) has achieved huge empirical successes in both continuous [36, 18] and discrete [39, 26] problem settings with on-policy [52, 54] and off-policy [13, 22, 23] algorithms. Especially in the continuous control domain, interpreting RL as probabilistic inference [60, 61] has yielded many kinds of algorithms with strong empirical performances [34, 50, 51, 12, 29, 21, 16, 24].

Recently, there has been a series of off-policy algorithms derived from this perspective for learning policies with function approximations [2, 22, 48]. Notably, Soft Actor Critic (SAC) [22, 23], based on a maximum entropy objective and soft Q-function, significantly outperforms on-policy [52, 54] and off-policy [36, 18, 13] methods. Maximum a posteriori Policy Optimisation (MPO) [2],

---

<sup>1</sup>The implementation is available at <https://github.com/frt03/inference-based-rl>.

inspired by REPS [50], employs a pseudo-likelihood objective, and achieves high sample-efficiency and fast convergence compared to the variety of policy gradient methods [36, 54, 7]. Similar to MPO, Advantage Weighted Regression (AWR) [48], and its variant, Advantage Weighted Actor-Critic (AWAC) [42], also employ the pseudo-likelihood objective weighted by the exponential of advantages, and reports more stable performance than baselines both in online and offline [35] settings.

While these inference-based algorithms have similar derivations to each other, their empirical performances have large gaps among them when evaluated on the standard continuous control benchmarks, such as OpenAI Gym [6] or DeepMind Control Suite [58]. Critically, as each algorithm has unique low-level implementation or code design decisions – such as value estimation techniques, action distribution for the policy, and network architectures – aside from high-level algorithmic choices, it is difficult to exactly identify the causes of these performance gaps as algorithmic or implementational.

In this paper, we first derive MPO, AWR, and SAC from a single objective function, through either Expectation-Maximization (EM) or KL minimization, mathematically clarifying the algorithmic connections among the recent state-of-the-art off-policy actor-critic algorithms. This unified derivation allows us to precisely identify implementation techniques and code details for each algorithm, which are residual design choices in each method that are generally transferable to other algorithms. To reveal the sources of the performance gaps, we experiment with carefully-selected ablations of these identified implementation techniques and code details, such as tanh-squashed Gaussian policy, clipped double Q-learning [13], and network architectures. Specifically, we keep the high-level algorithmic designs while normalizing the implementation designs, enabling proper algorithmic comparisons. Our empirical results successfully distinguish between highly co-adapted design choices and no-co-adapted ones<sup>2</sup>. We identified that clipped double Q-learning and tanh-squashed policies, the sources of SoTA performance of SAC, are highly co-adapted, specific to KL-minimization-based method, SAC, and difficult to transfer and benefit in EM-based methods, MPO or AWR. In contrast, we discover that ELU [8] and layer normalization [4], the sources of SoTA performance of MPO, are transferable choices from MPO that also significantly benefit SAC. We hope our work can inspire more future works to precisely decouple algorithmic innovations from implementation or code details, which allows exact sources of performance gains to be identified and algorithmic researches to better build on one another.

## 2 Related Work

**Inference-based RL algorithms** RL as probabilistic inference has been studied in several prior contexts [60, 61, 34, 11, 57, 45], but many recently-proposed algorithms [2, 22, 48] are derived separately and their exact relationships are difficult to get out directly, due to mixing of algorithmic and implementational details, inconsistent implementation choices, environment-specific tunings, and benchmark differences. Our work organizes them as a unified policy iteration method, to clarify their exact mathematical algorithmic connections and tease out subtle, but important, implementation differences. We center our analyses around MPO, AWR, and SAC, because they are representative algorithms that span both EM-based [49, 50, 43, 44, 1, 56, 42] and KL-control-based [59, 51, 12, 29, 21, 33, 32] RL and achieve some of the most competitive performances on popular benchmarks [6, 58]. REPS [50], an EM approach, inspired MPO, AWR, and our unified objective in Eq. 1, while Soft Q-learning [21], a practical extension of KL control to continuous action space through Liu and Wang [38], directly led to the development of SAC.

**Meta analyses of RL algorithms** While many papers propose novel algorithms, some recent works focused on meta analyses of some of the popular algorithms, which attracted significant attention due to these algorithms’ high-variance evaluation performances, reproducibility difficulty [9, 28, 65], and frequent code-level optimizations [25, 63, 10, 3]. Henderson et al. [25] empirically showed how these RL algorithms have inconsistent results across different official implementations and high variances even across runs with the same hyper-parameters, and recommended a concrete action item for the community – use more random seeds. Tucker et al. [63] show that high performances of action-dependent baselines [19, 17, 37, 20, 67] were more directly due to different subtle implementation choices. Engstrom et al. [10] focus solely on PPO and TRPO, two on-policy algorithms, and discuss

<sup>2</sup>We here regard as *co-adaptation* the indispensable implementation or code decisions that do not stem directly from the conceptual algorithmic development, but from empirical considerations.

Method	Algorithm	Implementation				
		$\pi_q$ update	$\pi_p$ update	$\mathcal{G}$	$\mathcal{G}$ estimate	$\pi_\theta$
MPO	EM	Analytic + TR	SG + TR	$Q^{\pi_p}$	Retrace(1)	$\pi_p = \mathcal{N}(\mu_\theta(s), \Sigma_\theta(s))$
AWR	EM	Analytic	Mixture + SG	$A^{\pi_p}$	TD( $\lambda$ )	$\pi_p = \mathcal{N}(\mu_\theta(s), \Sigma)$
AWAC	EM	Analytic	Mixture + SG	$Q^{\pi_p}$	TD(0)	$\pi_p = \mathcal{N}(\mu_\theta(s), \Sigma_\theta)$
SAC	KL	SG	(Fixed to Unif.)	$Q^{\pi_q}_{\text{soft}}$	TD(0) + TD3	$\pi_q = \text{Tanh}(\mathcal{N}(\mu_\theta(s), \Sigma_\theta(s)))$
PoWER	EM	Analytic	Analytic	$\eta \log Q^{\pi_p}$	TD(1)	$\pi_p = \mathcal{N}(\mu_\theta(s), \Sigma_\theta(s))$
RWR	EM	Analytic	SG	$\eta \log r$	–	$\pi_p = \mathcal{N}(\mu_\theta(s), \Sigma)$
REPS	EM	Analytic	$\pi_q$	$A^{\pi_p}$	TD(0)	$\pi_p = \text{Softmax}$
UREX	EM	Analytic	SG	$Q^{\pi_p}$	TD(1)	$\pi_p = \text{Softmax}$
V-MPO	EM	Analytic + TR	SG + TR	$A^{\pi_p}$	$n$ -step TD	$\pi_p = \mathcal{N}(\mu_\theta(s), \Sigma_\theta(s))$
TRPO	KL	TR	$\pi_q$	$A^{\pi_p}$	TD(1)	$\pi_q = \mathcal{N}(\mu_\theta(s), \Sigma_\theta)$
PPO	KL	SG + TR	$\pi_q$	$A^{\pi_p}$	GAE	$\pi_q = \mathcal{N}(\mu_\theta(s), \Sigma_\theta)$
DDPG*	KL	SG	(Fixed)	$Q^{\pi_q}$	TD(0)	$\pi_q = \mu_\theta(s)$
TD3*	KL	SG	(Fixed)	$Q^{\pi_q}$	TD(0) + TD3	$\pi_q = \mu_\theta(s)$

Table 1: Taxonomy based on the components of inference-based off-policy algorithms: MPO [2], AWR [48], AWAC [42], SAC [22], and other algorithms (see Appendix B). We follow the notation of Sec. 3 & 4. We characterize them with the algorithm family (EM or KL), how policies are updated ( $\pi_q$  and  $\pi_p$ ; SG stands for stochastic-gradient-based, and TR stands for trust-region-based), the choice of  $\mathcal{G}(\cdot)$ , how  $\mathcal{G}$  is estimated, and the parameterization of the policy. While the advantage function just can be interpreted as Q-function with baseline subtraction, we explicitly write  $A^\pi$  when the state-value function is parameterized, not Q-function. (\*Note that DDPG and TD3 are not “inference-based”, but can be classified as KL control variants.)

how code-level optimizations, instead of the claimed algorithmic differences, actually led more to PPO’s superior performances. Andrychowicz et al. [3] describes low-level (e.g. hyper-parameter choice, and regularization) and high-level (e.g. policy loss) design choices in on-policy algorithms affects the performance of PPO by showing results of large-scale evaluations.

In contrast to those prior works that mainly focus on a single family of on-policy algorithms, PPO and TRPO, and evaluating their implementation details alone, our work focuses on two distinct families of off-policy algorithms, and more importantly, presents unifying mathematical connections among independently-proposed state-of-the-art algorithms. Our experiments demonstrate how *some* implementation choices in Table 1 and code details are co-evolved with algorithmic innovations and/or have non-trivial effects on the performance of off-policy inference-based methods.

### 3 Preliminaries

We consider a Markov Decision Process (MDP) defined by state space  $\mathcal{S}$ , action space  $\mathcal{A}$ , state transition probability function  $p : \mathcal{S} \times \mathcal{A} \times \mathcal{S} \rightarrow [0, \infty)$ , initial state distribution  $p_1 : \mathcal{S} \rightarrow [0, \infty)$ , reward function  $r : \mathcal{S} \times \mathcal{A} \rightarrow \mathbb{R}$ , and discount factor  $\gamma \in [0, 1)$ . Let  $R_t$  denote a discounted return  $\sum_{u=t}^{\infty} \gamma^{u-t} r(s_u, a_u)$ . We assume the standard RL setting, where the agent chooses actions based on a parametric policy  $\pi_\theta$  and seeks for parameters that maximize the expected return  $\mathbb{E}_{\pi_\theta} [R_1]$ . Value functions for a policy  $\pi$  are the expected return conditioned by a state-action pair or a state, that is,  $Q^\pi(s_t, a_t) := \mathbb{E}_\pi [R_t | s_t, a_t]$ , and  $V^\pi(s_t) := \mathbb{E}_\pi [R_t | s_t]$ . They are called the state-action-value function (Q-function), and state-value function, respectively. The advantage function [5] is defined as  $A^\pi(s, a) := Q^\pi(s, a) - V^\pi(s)$ . The Q-function for a policy  $\pi$  is the unique fixed point of the Bellman operator  $\mathcal{T}^\pi$  defined by  $\mathcal{T}^\pi Q(s, a) = r(s, a) + \int \pi(a' | s') p(s' | s, a) Q(s', a') ds' da'$  for any function  $Q : \mathcal{S} \times \mathcal{A} \rightarrow \mathbb{R}$ . We denote a trajectory or successive state-action sequence as  $\tau := (s_1, a_1, s_2, a_2, \dots)$ . We also define an unnormalized state distribution under the policy  $\pi$  by  $d_\pi(s) = \sum_{t=1}^{\infty} \gamma^t p(s_t = s | \pi)$ .

**Inference-based Methods** For simplicity, we consider a finite-horizon MDP with a time horizon  $T$  for the time being. As a result, a trajectory  $\tau$  becomes a finite length:  $\tau := (s_1, a_1, \dots, s_{T-1}, a_{T-1}, s_T)$ .

As in previous works motivated by probabilistic inference [34, 2], we introduce to the standard graphical model of an MDP a binary event variable  $\mathcal{O}_t \in \{0, 1\}$ , which represents whether the action in time step  $t$  is *optimal* or not. To derive the RL objective, we consider the marginal log-likelihood  $\log \Pr(\mathcal{O} = 1 | \pi_p)$ , where  $\pi_p$  is a policy. Note that  $\mathcal{O} = 1$  means  $\mathcal{O}_t = 1$  for every time step. As is

well known, we can decompose this using a variational distribution  $q$  of a trajectory as follows:

$$\begin{aligned} \log \Pr(\mathcal{O} = 1 | \pi_p) &= \mathbb{E}_q \left[ \log \Pr(\mathcal{O} = 1 | \tau) - \log \frac{q(\tau)}{p(\tau)} + \log \frac{q(\tau)}{p(\tau | \mathcal{O} = 1)} \right] \\ &= \mathcal{J}(p, q) + D_{KL}(q(\tau) || p(\tau | \mathcal{O} = 1)), \end{aligned}$$

where  $\mathcal{J}(p, q) := \mathbb{E}_q [\log \Pr(\mathcal{O} = 1 | \tau)] - D_{KL}(q(\tau) || p(\tau))$  is the evidence lower bound (ELBO). Inference-based methods aim to find the parametric policy which maximizes the ELBO  $\mathcal{J}(p, q)$ .

There are several algorithmic design choices for  $q$  and  $\Pr(\mathcal{O} = 1 | \tau)$ . Since any  $q$  is valid, a popular choice is the one that factorizes in the same way as  $p$ , that is,

$$p(\tau) = p(s_1) \prod_t p(s_{t+1} | s_t, a_t) \pi_p(a_t | s_t), \quad q(\tau) = p(s_1) \prod_t p(s_{t+1} | s_t, a_t) \pi_q(a_t | s_t),$$

where  $\pi_p$  is a prior policy, and  $\pi_q$  is a variational posterior policy. We may also choose which policy ( $\pi_p$  or  $\pi_q$ ) to parameterize. As for  $\Pr(\mathcal{O} = 1 | \tau)$ , the most popular choice is the following one [21, 22, 2, 34, 48]:

$$\Pr(\mathcal{O} = 1 | \tau) \propto \exp \left( \sum_{t=1}^T \eta^{-1} \mathcal{G}(s_t, a_t) \right),$$

where  $\eta > 0$  is a temperature, and  $\mathcal{G}$  is a function over  $\mathcal{S} \times \mathcal{A}$ , such as an immediate reward function  $r$ , Q-function  $Q^\pi$ , and advantage function  $A^\pi$ . While we employ  $\exp(\cdot)$  in the present paper, there are alternatives [46, 47, 55, 66]: for example, Siegel et al. [55] and Wang et al. [66] consider an indicator function  $f : x \in \mathbb{R} \mapsto \mathbb{1}[x \geq 0]$ , whereas Oh et al. [46] consider the rectified linear unit  $f : x \in \mathbb{R} \mapsto \max\{x, 0\}$ .

Incorporating these design choices, we can rewrite the ELBO  $\mathcal{J}(p, q)$  in a more explicit form as;

$$\mathcal{J}(\pi_p, \pi_q) = \sum_{t=1}^T \mathbb{E}_q \left[ \eta^{-1} \mathcal{G}(s_t, a_t) - D_{KL}(\pi_q(\cdot | s_t) || \pi_p(\cdot | s_t)) \right].$$

In the following section, we adopt this ELBO and consider its relaxation to the infinite-horizon setting. Then, starting from it, we derive MPO, AWR, and SAC.

## 4 A Unified View of Inference-based Off-Policy Actor-Critic Algorithms

In Sec. 3, we provided the explicit form of the ELBO  $\mathcal{J}(\pi_p, \pi_q)$ . However, in practice, it is difficult to maximize it as the expectation  $\mathbb{E}_q$  depends on  $\pi_q$ . Furthermore, since we are interested in a finite-horizon setting, we replace  $\sum_{t \in [T]} \mathbb{E}_q$  with  $\mathbb{E}_{d_\pi(s)}$ . Note that the latter expectation  $\mathbb{E}_{d_\pi(s)}$  is taken with the unnormalized state distribution  $d_\pi$  under an arbitrary policy  $\pi$ . This is commonly assumed in previous works [2, 22]. This relaxation leads to the following optimization:

$$\max_{\pi_p, \pi_q} \mathcal{J}(\pi_p, \pi_q) \text{ s.t. } \int d_\pi(s) \int \pi_p(a|s) \, dads = 1 \text{ and } \int d_\pi(s) \int \pi_q(a|s) \, dads = 1, \quad (1)$$

where  $\mathcal{J}(\pi_p, \pi_q) = \mathbb{E}_{d_\pi(s)} [\eta^{-1} \mathcal{G}(s, a) - D_{KL}(\pi_q || \pi_p)]$ . With this objective, we can regard recent popular SoTA off-policy algorithms, MPO [2], AWR [48], and SAC [22] as variants of a unified policy iteration method. The components are summarized in Table 1. We first explain how these algorithms can be grouped into two categories of approaches for solving Eq. 1, and then we elaborate additional implementation details each algorithm makes.

### 4.1 Unified Policy Iteration: Algorithmic Perspective

Eq. 1 allows the following algorithmic choices: how or if to parameterize  $\pi_p$  and  $\pi_q$ ; what optimizer to use for them; and if to optimize them jointly, or individually while holding the other fixed. We show that the algorithms in Table 1 can be classified into two categories: Expectation-Maximization control (EM control) and direct Kullback-Leibler divergence minimization control (KL control).

#### 4.1.1 Expectation-Maximization (EM) Control

This category subsumes MPO [2] (similarly REPS [50]), AWR [48], and AWAC [42], and we term it *EM control*. At high level, the algorithm non-parametrically solves for the variational posterior  $\pi_q$  while holding the parametric prior  $\pi_p = \pi_{\theta_p}$  fixed (E-Step), and then optimize  $\pi_p$  holding the new  $\pi_q$  fixed (M-Step). This can be viewed as either a generic EM algorithm and as performing coordinate ascent on Eq. 1. We denote  $\theta_p$  and  $\pi_q$  after iteration  $k$  of EM steps by  $\theta_p^{(k)}$  and  $\pi_q^{(k)}$ , respectively.

In **E-step** at iteration  $k$ , we force the variational posterior policy  $\pi_q^{(k)}$  to be close to the optimal posterior policy, i.e., the maximizer of the ELBO  $\mathcal{J}(\pi_{\theta_p^{(k-1)}}, \pi_q)$  with respect to  $\pi_q$ . EM control converts the hard-constraint optimization problem in Eq. 1 to solving the following Lagrangian,

$$\begin{aligned} \mathcal{J}(\pi_q, \beta) = & \int d\pi(s) \int \pi_q(a|s) \eta^{-1} \mathcal{G}(s, a) \, dads \\ & - \int d\pi(s) \int \pi_q(a|s) \log \frac{\pi_q(a|s)}{\pi_{\theta_p^{(k-1)}}(a|s)} \, dads + \beta \left( 1 - \int d\pi(s) \int \pi_q(a|s) \, dads \right). \end{aligned} \quad (2)$$

We analytically obtain the solution of Eq. 2,

$$\pi_q^{(k)}(a|s) = Z(s)^{-1} \pi_{\theta_p^{(k-1)}}(a|s) \exp(\eta^{-1} \mathcal{G}(s, a)),$$

where  $Z(s)$  is the partition function.

In **M-Step** at iteration  $k$ , we maximize the ELBO  $\mathcal{J}(\pi_q^{(k)}, \pi_p)$  with respect to  $\pi_p$ . Considering the optimization with respect to  $\pi_p$  in Eq. 1 results in *forward* KL minimization, which is often referred to as a pseudo-likelihood or policy projection objective,

$$\max_{\theta_p} \mathbb{E}_{d_{\pi(s)} \pi_q^{(k)}(a|s)} [\log \pi_{\theta_p}(a|s)] = \max_{\theta_p} \mathbb{E}_{d_{\pi(s)} \pi_{\theta_p^{(k-1)}}(a|s)} \left[ \frac{\log \pi_{\theta_p}(a|s)}{Z(s)} \exp(\eta^{-1} \mathcal{G}(s, a)) \right], \quad (3)$$

where we may approximate  $Z(s) \approx \frac{1}{M} \sum_{j=1}^M \exp(\eta^{-1} \mathcal{G}(s, a_j))$  with  $a_j \sim \pi_{\theta_p^{(k-1)}}(\cdot|s)$  in practice.

#### 4.1.2 Direct Kullback-Leibler (KL) Divergence Minimization Control

In contrast to the EM control in Sec. 4.1.1, we only optimize the variational posterior  $\pi_q$  while holding the prior  $\pi_p$  fixed. In this scheme,  $\pi_q$  is parameterized, so we denote it as  $\pi_{\theta_q}$ . This leads to *KL control* [59, 62, 51, 12, 29, 21].

Equivalent to E-step in Sec. 4.1.1, we force the variational posterior policy  $\pi_{\theta_q}$  to be close to the optimal posterior policy, i.e, the maximizer of  $\mathcal{J}(\pi_p, \pi_q)$  with respect to  $\pi_q$ . The difference is that instead of analytically solving  $\mathcal{J}(\pi_p, \pi_q)$  for  $\pi_q$ , we optimize  $\mathcal{J}(\pi_p, \pi_{\theta_q})$  with respect to  $\theta_q$ , which results in the following objective,

$$\max_{\theta_q} \mathbb{E}_{d_{\pi(s)} \pi_{\theta_q}(a|s)} \left[ \eta^{-1} \mathcal{G}(s, a) - \log \frac{\pi_{\theta_q}(a|s)}{\pi_p(a|s)} \right].$$

#### 4.1.3 “Optimal” Policies of EM and KL Control

While we formulate EM and KL control in a unified framework, we note that they have a fundamental difference in their definition of “optimal” policies. KL control fixes  $\pi_p$  and converges to a *regularized-optimal* policy in an exact case [15, 64]. In contrast, EM control continues updating both  $\pi_p$  and  $\pi_q$ , resulting in convergence to the *standard optimal* policy in an exact case [51]. We also note that EM control solves KL control as a sub-problem; for example, the first E-step exactly corresponds to a KL control problem, except for the policy parameterization.

## 4.2 Unified Policy Iteration: Implementation Details

In this section, we explain the missing pieces of MPO, AWR, and SAC in Sec. 4.1. Additionally, we also describe the details of other algorithms [30, 49, 50, 41, 56, 36, 13, 52, 54] from the EM and KL control perspective. See Appendix B for the details.

### 4.2.1 MPO

**Algorithm** MPO closely follows the EM control scheme explained in Sec. 4.1.1, wherein  $\pi_p = \pi_{\theta_p}$  is parametric, and  $\pi_q$  is non-parametric.

**Implementation [ $\pi_q$  Update]** This corresponds to the E-step. MPO uses a trust-region (TR) method. Concretely, it replaces the reverse KL penalty (second term) in the Lagrangian (Eq. 2) with a constraint and analytically solves it for  $\pi_q$ . As a result,  $\eta$  is also optimized during the training by minimizing the dual of Eq. 2, which resembles REPS [50]:

$$g(\eta) = \eta\epsilon + \eta \log \mathbb{E}_{d_{\pi(s)}\pi_{\theta_p^{(k-1)}}(a|s)} \left[ \exp \left( \eta^{-1} Q^{\pi_{\theta_p^{(k-1)}}}(s, a) \right) \right].$$

**[ $\pi_p$  Update]** This corresponds to the M-step. MPO uses a combination of Stochastic Gradient (SG) ascent and trust-region method based on a forward KL divergence similarly to TRPO [52]. Concretely, it obtains  $\theta_p^{(k)}$  by maximizing the objective (Eq. 3) with respect to  $\theta_p$  subject to  $\mathbb{E}_{d_{\pi(s)}}[D_{KL}(\pi_{\theta_p^{(k-1)}}(\cdot|s) || \pi_{\theta_p}(\cdot|s))] \leq \epsilon$ . MPO further decompose this KL divergence to two terms, assuming Gaussian policies; one term includes only the mean vector of  $\pi_{\theta_p}(\cdot|s)$ , and the other includes only its covariance matrix. Abdolmaleki et al. [2] justify this as a log-prior of MAP estimation, which is assumed as a second-order approximation of KL divergence.

**[ $\mathcal{G}$  and  $\mathcal{G}$  Estimate]** MPO uses the Q-function of  $\pi_{\theta_p^{(k-1)}}$  as  $\mathcal{G}$  in the  $k$ -th E-step. It originally uses the Retrace update [40], while its practical implementation [27] uses a single-step Bellman update.

**[ $\pi_{\theta}$ ]** For a parameterized policy, MPO uses a Gaussian distribution with state-dependent mean vector and diagonal covariance matrix. The trust-region method in MPO’s M-step heavily relies on this Gaussian assumption. Since a Gaussian distribution has an infinite support, MPO has a penalty term in its policy loss function that forces the mean of the policy to stay within the range of action space.

### 4.2.2 AWR and AWAC

**Algorithm** AWR slightly deviates from the EM control. In the M-step, AWR simply set  $Z(s)$  to 1.

**Implementation [ $\pi_q$  Update]** This corresponds the E-step. AWR and AWAC analytically solves the Lagrangian (Eq. 2). In contrast to MPO, they don’t use trust-region method.

**[ $\pi_p$  Update]** This corresponds to the M-step. At iteration  $k$ , AWR uses an average of all previous policies  $\tilde{\pi}_{p^k} := \frac{1}{k} \sum_{j=0}^{k-1} \pi_{\theta_p^{(j)}}$  instead of  $\pi_{\theta_p^{(k-1)}}$  (cf. Eq. 3). In practice, the average policy  $\tilde{\pi}_{p^k}$  is replaced by samples of actions from a replay buffer, which stores action samples of previous policies.

**[ $\mathcal{G}$  and  $\mathcal{G}$  Estimate]** AWR uses the advantage function of  $\tilde{\pi}_{p^k}$  as  $\mathcal{G}$  in the  $k$ -th E-step, and learns the state-value function of  $\pi_{\theta_p^{(k-1)}}$  with TD( $\lambda$ ) [53]. Due to its choice of  $\tilde{\pi}_{p^k}$ , this avoids importance corrections [40]. In contrast, AWAC estimates the advantage via the Q-function with TD(0).

**[ $\pi_{\theta}$ ]** For a parameterized policy, both AWR and AWAC use a Gaussian distribution with state-dependent mean vector and state-independent diagonal covariance matrix (a constant one for AWR). As in MPO, they uses a penalty term to keep the mean of the policy within the range of action space.

### 4.2.3 SAC

**Algorithm** Contrary to MPO and AWR, SAC follows the KL control scheme explained in Sec. 4.1.2, wherein the variational posterior policy  $\pi_q = \pi_{\theta_q}$  is parameterized, and the prior policy  $\pi_p$  is fixed to the uniform distribution over the action space  $\mathcal{A}$ . SAC uses as  $\mathcal{G}$  a soft Q-function:

$$Q_{\text{soft}}^{\pi_{\theta_q}}(s_t, a_t) := r(s_t, a_t) + \gamma \mathbb{E}_{\pi_{\theta_q}} \left[ V_{\text{soft}}^{\pi_{\theta_q}}(s_{t+1}) \right],$$

$$V_{\text{soft}}^{\pi_{\theta_q}}(s_t) := V^{\pi_{\theta_q}}(s_t) + \mathbb{E}_{\pi_{\theta_q}} \left[ \sum_{u=t}^{\infty} \gamma^{u-t} \eta \mathcal{H}(\pi_{\theta_q}(\cdot|s_t)) | s_t \right],$$

with  $\mathcal{H}(\pi_{\theta_q}(\cdot|s_t))$  being  $-\mathbb{E}_{\pi_{\theta_q}}[\log \pi_{\theta_q}(a_t|s_t)|s_t]$ .

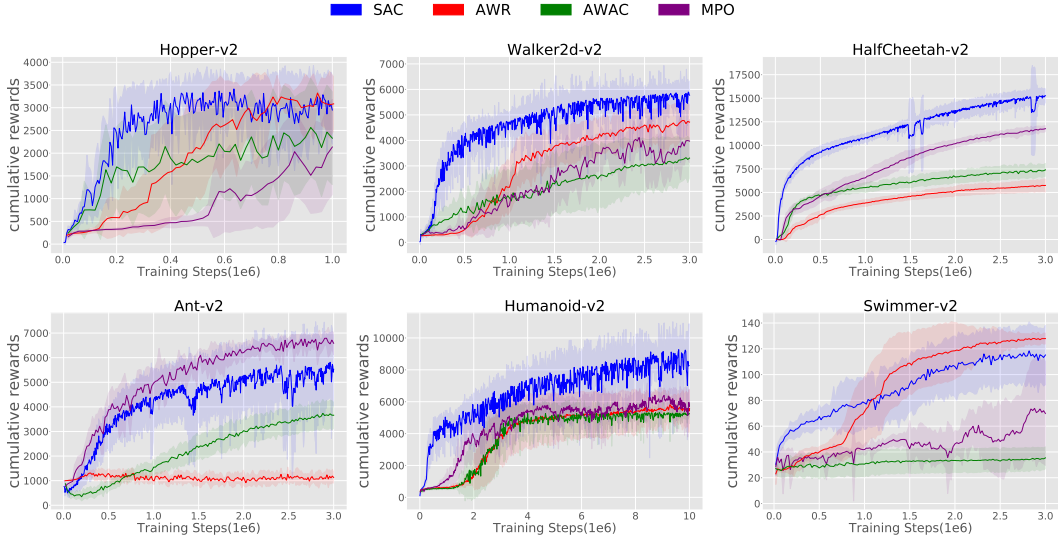


Figure 1: Benchmarking results on OpenAI Gym MuJoCo locomotion environments. All methods are run with 10 random seeds. SAC seems to perform consistently better.

**Implementation [ $\pi_q$  and  $\pi_p$  Update]** SAC performs stochastic gradient (SG) ascent updates of only  $\pi_q$ , where the objective function is shown in Eq. 1. SAC has no operation equivalent to M-step in MPO and AWR, since it keeps the prior policy  $\pi_p$  to the uniform distribution.

Similar to the temperature tuning in MPO, Haarnoja et al. [23] consider the dual function of entropy-constrained Lagrangian and treat the temperature  $\eta$  as a Lagrange multiplier, which results in,

$$g(\eta) = -\eta\bar{\mathcal{H}} - \eta\mathbb{E}_{d_{\pi}(s)}\pi_{\theta_q}(a|s) [\log \pi_{\theta_q}(a|s)],$$

where  $\bar{\mathcal{H}}$  is the target entropy to ensure that the entropy of the policy should be larger than it.

**[ $\mathcal{G}$  and  $\mathcal{G}$  Estimate]** SAC uses  $Q_{\text{soft}}^{\pi_{\theta_q}}$  as  $\mathcal{G}$ , and TD(0)-like algorithm based on this soft Q-function. In policy evaluation, clipped double Q-learning [13], which retains multiple Q-functions (typically two) and takes the minimum, is employed to suppress the overestimation of Q value.

**[ $\pi_{\theta}$ ]** The policy of SAC is a squashed Gaussian distribution: SAC first samples a random variable  $u$  from a Gaussian distribution  $\mathcal{N}(\mu_{\theta}(s), \Sigma_{\theta}(s))$  with state-dependent mean vector and diagonal covariance; then, it applies the tanh function to  $u$  and obtain the action  $a \in [-1, 1]^{|A|}$ . (If a dimension of the action space is not  $[-1, 1]$ , an appropriate scaling and shift by an affine function is applied after the squashing.) Tanh squashing prevents out-of-bounds action.

### 4.3 Empirical Comparison

To evaluate the empirical performance of these off-policy algorithms (MPO, AWR, AWAC, and SAC), we compare their performances on Open AI Gym MuJoCo environments, namely, Hopper, Walker2d, HalfCheetah, Ant, Humanoid, and Swimmer, following Haarnoja et al. [23]. We reproduce all algorithms based on pytorch RL library [14], referring their original implementations [22, 48, 42, 27]. Figure 1 shows that SAC outperforms others in four environments (Hopper, Walker2d, HalfCheetah, and Humanoid), while MPO in Ant and AWR in Swimmer achieves the best performance. Generally, SAC seems to perform consistently better. We extensively evaluate MPO, AWR, and SAC on the 28 tasks on DeepMind Control Suite and 3 MuJoCo manipulation tasks. See Appendix C and D for the details.

## 5 Evaluation on Implementational Choices

In Sec. 4.3, SAC shows notable results in most environments, while we revealed that the derivation and formulation of those methods resemble each other. To specify the effect of each implementational

	<b>SAC (D)</b>	<b>SAC (S)</b>	<b>AWAC (D)</b>	<b>AWAC (S)</b>	<b>MPO (D)</b>	<b>MPO (S)</b>
Hopper-v2	<b>3013 ± 602</b>	1601 ± 733	2329 ± 1020	2540 ± 755	2352 ± 959	2136 ± 1047
Walker2d-v2	<b>5820 ± 411</b>	1888 ± 922	3307 ± 780	3662 ± 712	4471 ± 281	3972 ± 849
HalfCheetah-v2	15254 ± 751	<b>15701 ± 630</b>	7396 ± 677	7226 ± 449	12028 ± 191	11769 ± 321
Ant-v2	5532 ± 1266	1163 ± 1326	3659 ± 523	3008 ± 375	<b>7179 ± 190</b>	6584 ± 455
Humanoid-v2	<b>8081 ± 1149</b>	768 ± 215	5243 ± 200	2738 ± 982	6858 ± 373	5709 ± 1081
Swimmer-v2	114 ± 21	<b>143 ± 3</b>	35 ± 8	38 ± 7	69 ± 29	70 ± 40

Table 2: Ablation of Clipped Double Q-Learning. (D) denotes algorithms with clipped double Q-learning, and (S) denotes without it. We test original SAC (D), AWAC (D), MPO (S) and some variants; SAC without clipped double Q (S), AWAC (S), and MPO with clipped double Q (D). SAC (S) beats SAC (D) in HalfCheetah and Swimmer, while it fails in Hopper, Walker, Ant and Humanoid, which implies that SAC (S) obtains a highly exploratory policy, since it fails in termination environments. The learning curves are shown in Appendix F.

or code detail on the performance, we experiment with extensive and careful one-by-one ablations on; (1) clipped double Q-learning, (2) action distribution for the policy, (3) activation and normalization, and (4) network size. The former two correspond to implementation details (the choice of  $\mathcal{G}$  estimate and the parameterization of the policy), and the latter two correspond to code details (see Appendix G for further experiments on other implementation details, such as  $\pi_p$  update or the choice of  $\mathcal{G}$ ). We also conclude several recommendations for the practitioners (Table 6).

### 5.1 Clipped Double Q-Learning

We hypothesize that clipped double Q-learning has a large effect on the notable performance of SAC, and could be transferable in EM control methods. To verify this, we test the effect of clipped double Q-learning. Instead of AWR, here we evaluate AWAC since it uses Q-function. Table 2 shows that single-Q SAC outperforms original one in HalfCheetah and Swimmer that do not have the termination of the episode, while struggles to learn in Hopper, Walker, Ant and Humanoid that have the episodic termination conditions. A hypothesis is that single-Q SAC obtains a more exploratory policy due to larger overestimation bias, which can help in environments where explorations are safe, but hurt in environments where reckless explorations lead to immediate terminations. In contrast, clipped double Q-learning does not help MPO or AWAC as significantly as SAC; most results do not change or lead to slight improvements over the originals. This suggests that clipped double Q-learning might be a co-dependent and indispensable choice to KL control methods.

**Recommendation** Use clipped double Q-learning as a default choice, but you can omit it in EM control methods or non-terminal environments, such as HalfCheetah or Swimmer.

### 5.2 Action Distribution for the Policy

Another hypothesis is that the tanh-squashed policy (last column in Table 1) is an important and transferable design choice. We compare SAC without tanh transform (with MPO action penalty instead) to the original one, which results in drastic degradation (Table 3). This can be caused by the maximum entropy objective that encourages maximizing the covariance. These observations suggest that the high performance of SAC seems to highly depend on the implementational choice of the policy distribution. In contrast, MPO and AWR with tanh squashing don’t enjoy such large performance gain, or achieve worse cumulative rewards. This also suggests that tanh-squashed policy might be highly co-adapted in SAC and less transferable to EM control methods. Note that for EM control, we must clip the actions to keep them within the supports of distributions;  $a \in [-1 + \epsilon, 1 - \epsilon]^{|A|}$ . We found that no clipping cause significant numerical instability. See Appendix H for the details.

**Recommendation** Use the original distributions for each algorithm. If you use the tanh-squashed Gaussian in EM control methods, clip the action to be careful for the numerical instability.

### 5.3 Activation and Normalization

The implementation of MPO [27] has some code-level detailed choices; ELU activation [8] and layer normalization [4]. We hypothesize that these, sometimes unfamiliar, code details in practical implementation stabilize the learning process, and contribute to the performance of MPO most.



	SAC (w/)	SAC (w/o)	AWR (w/)	AWR (w/o)	MPO (w/)	MPO (w/o)
Hopper-v2	3013 ± 602	6 ± 10	2709 ± 905	<b>3085 ± 593</b>	2149 ± 849	2136 ± 1047
Walker2d-v2	<b>5820 ± 411</b>	−∞	3295 ± 335	4717 ± 678	3167 ± 815	3972 ± 849
HalfCheetah-v2	<b>15254 ± 751</b>	−∞	3653 ± 652	5742 ± 667	9523 ± 312	11769 ± 321
Ant-v2	5532 ± 1266	−∞	445 ± 106	1127 ± 224	2880 ± 306	<b>6584 ± 455</b>
Humanoid-v2	<b>8081 ± 1149</b>	108 ± 82 <sup>†</sup>	2304 ± 1629 <sup>†</sup>	5573 ± 1020	6688 ± 192	5709 ± 1081
Swimmer-v2	114 ± 21	28 ± 11	121 ± 3	<b>128 ± 4</b>	110 ± 42	70 ± 40

Table 3: Ablation of Tanh transformation (<sup>†</sup>numerical error happens during training). We test SAC without tanh squashing, AWR with tanh, and MPO with tanh. SAC without tanh transform results in drastic degradation of the performance, which can be caused by the maximum entropy objective that encourages the maximization of the covariance. In contrast, EM Control methods don’t enjoy the performance gain from the tanh-squashed policy, which seems a less transferable choice. The learning curves are shown in Appendix F.

	Hopper-v2	Walker2d-v2	HalfCheetah-v2	Ant-v2	Humanoid-v2	Swimmer-v2
<b>SAC</b>	3013 ± 602	<b>5820 ± 411</b>	15254 ± 751	5532 ± 1266	8081 ± 1149	114 ± 21
<b>SAC-E<sup>+</sup></b>	2337 ± 903	5504 ± 431	<b>15350 ± 594</b>	6457 ± 828	<b>8196 ± 892</b>	<b>146 ± 7</b>
<b>SAC-L<sup>+</sup></b>	2368 ± 179	5613 ± 762	13074 ± 2218	<b>7349 ± 176</b>	8146 ± 470	99 ± 18
<b>SAC-E<sup>+</sup>L<sup>+</sup></b>	1926 ± 417	5751 ± 400	12555 ± 1259	7017 ± 132	7687 ± 1385	143 ± 9
<b>MPO</b>	2136 ± 1047	3972 ± 849	11769 ± 321	6584 ± 455	5709 ± 1081	70 ± 40
<b>MPO-E<sup>-</sup></b>	2700 ± 879	3553 ± 1145	11638 ± 664	5917 ± 702	4870 ± 1917	108 ± 28
<b>MPO-L<sup>-</sup></b>	824 ± 250	2413 ± 1352	6064 ± 4596	2135 ± 2988	5039 ± 838	−∞
<b>MPO-E<sup>-</sup>L<sup>-</sup></b>	843 ± 168	1708 ± 663	−1363 ± 20965	807 ± 2351	5566 ± 787	−∞
<b>AWR</b>	3085 ± 593	4717 ± 678	5742 ± 667	1127 ± 224	5573 ± 1020	128 ± 4
<b>AWR-E<sup>+</sup></b>	1793 ± 1305	4418 ± 319	5910 ± 754	2288 ± 715	6708 ± 226	128 ± 4
<b>AWR-L<sup>+</sup></b>	2525 ± 1130	4900 ± 671	5391 ± 232	639 ± 68	5962 ± 376	129 ± 2
<b>AWR-E<sup>+</sup>L<sup>+</sup></b>	<b>3234 ± 118</b>	4906 ± 304	6081 ± 753	2283 ± 927	6041 ± 270	130 ± 1

Table 4: Incorporating ELU/layer normalization into SAC and AWR. E<sup>+</sup>/L<sup>+</sup> indicates adding, and E<sup>-</sup>/L<sup>-</sup> indicates removing ELU/layer normalization. Introducing layer normalization or ELU into SAC improves the performances in Ant (beating MPO), Swimmer (beating AWR), HalfCheetah, and Humanoid. AWR also shows the improvement in several tasks. MPO removing layer normalization largely drops its performance. Both code-level details seems transferable between EM and KL control methods.

Especially in Ant (Sec. 4.3), MPO significantly outperforms SAC. To investigate this much deeper, we add them into SAC or AWR and remove them from MPO, while maintaining the rest of the implementations. Table 4 shows that layer normalization can contribute to a significantly higher performance of SAC in Ant, and replacing ReLU with ELU also improves performance a lot in Swimmer, where AWR is the best in Figure 1. In contrast, the performance of MPO drastically collapsed when we just removed ELU and layer normalization. This observation suggests that these code-level choices are not only indispensable for MPO, but transferable and beneficial to both KL and EM control methods. Additionally, we tested incorporating ELU and layer normalization to SAC in 12 DM Control tasks where MPO outperformed SAC, and observed that they again often benefit SAC performances substantially. See Appendix C for the details.

**Recommendation** It is worth considering to replace the activation function from ReLU to ELU and incorporate the layer normalization, to achieve the best performance in several tasks. Both of them are transferable between EM and KL control methods.

## 5.4 Network Size

While on-policy algorithms such as PPO and TRPO can use the common network architecture as in prior works [10, 25], the architecture that works well in all the off-policy inference-based methods is still not obvious, and the RL community does not have agreed upon default choice. To validate the dependency on the networks among the inference-based methods, we exchange the size and number of hidden layers in the policy and value networks. We denote the network size of MPO ((256, 256, 256) for policy and (512, 512, 256) for value) as large (L), of SAC ((256, 256) for policy and value) as middle (M), and of AWR ((128, 64) for policy and value) as small (S) (see Appendix A for the details). Table 5 illustrates that SAC with large network seems to have better performance. However, as shown in Appendix F (Figure 8), the learning curve sometimes becomes unstable. While the certain degree of robustness to the network size is observed in SAC, EM control methods, MPO

	Hopper-v2	Walker2d-v2	HalfCheetah-v2	Ant-v2	Humanoid-v2	Swimmer-v2
<b>SAC (L)</b>	2486 ± 746	3188 ± 2115	<b>16528 ± 183</b>	<b>7495 ± 405</b>	<b>8255 ± 578</b>	118 ± 26
<b>SAC (M)</b>	3013 ± 602	<b>5820 ± 411</b>	15254 ± 751	5532 ± 1266	8081 ± 1149	114 ± 21
<b>SAC (S)</b>	<b>3456 ± 81</b>	4939 ± 284	12241 ± 400	3290 ± 691	7724 ± 497	59 ± 11
<b>MPO (L)</b>	2136 ± 1047	3972 ± 849	11769 ± 321	6584 ± 455	5709 ± 1081	70 ± 40
<b>MPO (M)</b>	661 ± 79	1965 ± 1426	−∞	5192 ± 538	6015 ± 771	81 ± 28
<b>MPO (S)</b>	430 ± 99	2055 ± 990	5003 ± 1567	3587 ± 957	4745 ± 1428	59 ± 28
<b>AWR (L)</b>	3221 ± 193	4688 ± 648	4360 ± 542	35 ± 43	665 ± 54	<b>133 ± 3</b>
<b>AWR (M)</b>	2816 ± 910	4826 ± 547	5538 ± 720	413 ± 117	3849 ± 1647	<b>133 ± 2</b>
<b>AWR (S)</b>	3085 ± 593	4717 ± 678	5742 ± 667	1127 ± 224	5573 ± 1020	128 ± 4

Table 5: The performance of each algorithm with different network size. (S) stands for the small network size from AWR, (M) for the middle network size from SAC, and (L) for the large network size from MPO. Generally, SAC, a KL control method seems more robust to the network size than EM control methods; MPO and AWR.

and AWR, seem fragile and more dependent on the specific network size. This trend is remarkable in MPO. AWR (M) or (L) also struggles to learn in high-dimensional state tasks, such as Ant (111 dim), or Humanoid (376 dim). The results also imply that, in contrast to on-policy methods [3], the network size in the off-policy inference-based methods seems a less transferable choice.

**Recommendation** For SAC, use medium size network. Large size will also work, but the learning curve might be unstable. For MPO, we strongly recommend to stick to large size, because it is very sensitive to the network size. For AWR, using small size is a better choice, especially in high-dimensional state tasks, such as Ant, or Humanoid.

## 6 Conclusion

In this work, we present a taxonomy of inference-based algorithms, and successfully identify algorithm-specific as well as algorithm-independent implementation details that cause substantial performance improvements. We first reformulated recent inference-based off-policy algorithms – such as MPO, AWR and SAC – into a unified mathematical objective and exhaustively clarified the algorithmic and implementational differences. Through precise ablation studies, we empirically show that implementation choices like tanh-squashed distribution and clipped double Q-learning are highly co-adapted to KL control methods (e.g. SAC), and difficult to benefit in EM control methods (e.g. MPO or AWR). As an example, the network architectures of inference-based off-policy algorithms, especially EM controls, seem more co-dependent than on-policy methods like PPO or TRPO, which therefore have significant impacts on the overall algorithm performances and need to be carefully tuned per algorithm. Such dependence of each algorithmic innovation on specific hand-tuned implementation details makes accurate performance gain attributions and cumulative build-up of research insights difficult. In contrast, we also find that some code-level implementation details, such as ELU and layer normalization, are not only indispensable choice to MPO, but also transferable and beneficial to SAC substantially. We hope our work can encourage more works that study precisely the impacts of algorithmic properties and empirical design choices, not only for one type of algorithms, but also across a broader spectrum of deep RL algorithms.

### Acknowledgements

We thank Yusuke Iwasawa, Masahiro Suzuki, Marc G. Bellemare, Ofir Nachum, and Sergey Levine for many fruitful discussions and comments. This work has been supported by the Mohammed bin Salman Center for Future Science and Technology for Saudi-Japan Vision 2030 at The University of Tokyo (MbSC2030).

	MPO	AWR	SAC
Clipped Double Q [5.1]	△	△	○
Tanh Gaussian [5.2]	△	△	○
ELU & LayerNorm [5.3]	○	○	○
Large Network [5.4]	○	△	○
Medium Network [5.4]	×	△	○
Small Network [5.4]	×	○	△

Table 6: Intuitive summary of the ablations. ○ stands for indispensable choice, △ stands for recommended choice, △ stands for not much different or worse choice than expected, and × stands for un-recommended choice. See **Recommendation** for the details.

## References

- [1] Abbas Abdolmaleki, Jost Tobias Springenberg, Jonas Degraeve, Steven Bohez, Yuval Tassa, Dan Belov, Nicolas Heess, and Martin Riedmiller. Relative entropy regularized policy iteration. *arXiv preprint arXiv:1812.02256*, 2018.
- [2] Abbas Abdolmaleki, Jost Tobias Springenberg, Yuval Tassa, Remi Munos, Nicolas Heess, and Martin Riedmiller. Maximum a posteriori policy optimisation. In *International Conference on Learning Representations*, 2018.
- [3] Marcin Andrychowicz, Anton Raichuk, Piotr Stańczyk, Manu Orsini, Sertan Girgin, Raphaël Marinier, Leonard Hussenot, Matthieu Geist, Olivier Pietquin, Marcin Michalski, Sylvain Gelly, and Olivier Bachem. What matters for on-policy deep actor-critic methods? a large-scale study. In *International Conference on Learning Representations*, 2021.
- [4] Jimmy Lei Ba, Jamie Ryan Kiros, and Geoffrey E Hinton. Layer normalization. *arXiv preprint arXiv:1607.06450*, 2016.
- [5] Leemon C Baird III. Advantage updating. Technical report, WRIGHT LAB WRIGHT-PATTERSON AFB OH, 1993.
- [6] Greg Brockman, Vicki Cheung, Ludwig Pettersson, Jonas Schneider, John Schulman, Jie Tang, and Wojciech Zaremba. Openai gym. *arXiv preprint arXiv:1606.01540*, 2016.
- [7] Kamil Ciosek and Shimon Whiteson. Expected policy gradients for reinforcement learning. *Journal of Machine Learning Research*, 2020.
- [8] Djork-Arné Clevert, Thomas Unterthiner, and Sepp Hochreiter. Fast and accurate deep network learning by exponential linear units (elus). In *International Conference on Learning Representations*, 2016.
- [9] Yan Duan, Xi Chen, Rein Houthoofd, John Schulman, and Pieter Abbeel. Benchmarking deep reinforcement learning for continuous control. In *International Conference on Machine Learning*, 2016.
- [10] Logan Engstrom, Andrew Ilyas, Shibani Santurkar, Dimitris Tsipras, Firdaus Janoos, Larry Rudolph, and Aleksander Madry. Implementation matters in deep rl: A case study on ppo and trpo. In *International Conference on Learning Representations*, 2019.
- [11] Matthew Fellows, Anuj Mahajan, Tim GJ Rudner, and Shimon Whiteson. Virel: A variational inference framework for reinforcement learning. In *Advances in Neural Information Processing Systems*, 2019.
- [12] Roy Fox, Ari Pakman, and Naftali Tishby. Taming the noise in reinforcement learning via soft updates. In *Conference on Uncertainty in Artificial Intelligence*, 2016.
- [13] Scott Fujimoto, Herke van Hoof, and David Meger. Addressing function approximation error in actor-critic methods. In *International Conference on Machine Learning*, 2018.
- [14] Yasuhiro Fujita, Prabhat Nagarajan, Toshiki Kataoka, and Takahiro Ishikawa. Chainerrl: A deep reinforcement learning library. *Journal of Machine Learning Research*, 2021.
- [15] Matthieu Geist, Bruno Scherrer, and Olivier Pietquin. A theory of regularized Markov decision processes. In *International Conference on Machine Learning*, 2019.
- [16] Seyed Kamyar Seyed Ghasemipour, Richard Zemel, and Shixiang Gu. A divergence minimization perspective on imitation learning methods. In *Conference on Robot Learning*, 2020.
- [17] Will Grathwohl, Dami Choi, Yuhuai Wu, Geoffrey Roeder, and David Duvenaud. Backpropagation through the void: Optimizing control variates for black-box gradient estimation. *arXiv preprint arXiv:1711.00123*, 2017.
- [18] Shixiang Gu, Timothy Lillicrap, Ilya Sutskever, and Sergey Levine. Continuous deep q-learning with model-based acceleration. In *International Conference on Machine Learning*, 2016.
- [19] Shixiang Gu, Timothy Lillicrap, Zoubin Ghahramani, Richard E. Turner, and Sergey Levine. Q-Prop: Sample-efficient policy gradient with an off-policy critic. In *International Conference on Learning Representations*, 2017.
- [20] Shixiang Gu, Timothy Lillicrap, Zoubin Ghahramani, Richard E. Turner, Bernhard Schölkopf, and Sergey Levine. Interpolated policy gradient: Merging on-policy and off-policy gradient estimation for deep reinforcement learning. In *Advances in Neural Information Processing Systems*, 2017.

- [21] Tuomas Haarnoja, Haoran Tang, Pieter Abbeel, and Sergey Levine. Reinforcement learning with deep energy-based policies. In *International Conference on Machine Learning*, 2017.
- [22] Tuomas Haarnoja, Aurick Zhou, Pieter Abbeel, and Sergey Levine. Soft actor-critic: Off-policy maximum entropy deep reinforcement learning with a stochastic actor. In *International Conference on Machine Learning*, 2018.
- [23] Tuomas Haarnoja, Aurick Zhou, Kristian Hartikainen, George Tucker, Sehoon Ha, Jie Tan, Vikash Kumar, Henry Zhu, Abhishek Gupta, Pieter Abbeel, and Sergey Levine. Soft actor-critic algorithms and applications. *arXiv preprint arXiv:1812.05905*, 2018.
- [24] Danijar Hafner, Pedro A Ortega, Jimmy Ba, Thomas Parr, Karl Friston, and Nicolas Heess. Action and perception as divergence minimization. *arXiv preprint arXiv:2009.01791*, 2020.
- [25] Peter Henderson, Riashat Islam, Philip Bachman, Joelle Pineau, Doina Precup, and David Meger. Deep reinforcement learning that matters. In *AAAI Conference on Artificial Intelligence*, 2017.
- [26] Matteo Hessel, Joseph Modayil, Hado Van Hasselt, Tom Schaul, Georg Ostrovski, Will Dabney, Dan Horgan, Bilal Piot, Mohammad Azar, and David Silver. Rainbow: Combining improvements in deep reinforcement learning. In *AAAI Conference on Artificial Intelligence*, 2018.
- [27] Matt Hoffman, Bobak Shahriari, John Aslanides, Gabriel Barth-Maron, Feryal Behbahani, Tamara Norman, Abbas Abdolmaleki, Albin Cassirer, Fan Yang, Kate Baumli, Sarah Henderson, Alex Novikov, Sergio Gómez Colmenarejo, Serkan Cabi, Caglar Gulcehre, Tom Le Paine, Andrew Cowie, Ziyu Wang, Bilal Piot, and Nando de Freitas. Acme: A research framework for distributed reinforcement learning. *arXiv preprint arXiv:2006.00979*, 2020.
- [28] Riashat Islam, Peter Henderson, Maziar Gomrokchi, and Doina Precup. Reproducibility of benchmarked deep reinforcement learning tasks for continuous control. *arXiv preprint arXiv:1708.04133*, 2017.
- [29] Natasha Jaques, Shixiang Gu, Dzmitry Bahdanau, José Miguel Hernández-Lobato, Richard E Turner, and Douglas Eck. Sequence tutor: Conservative fine-tuning of sequence generation models with kl-control. In *International Conference on Machine Learning*, 2017.
- [30] Jens Kober and Jan Peters. Policy search for motor primitives in robotics. In *Advances in neural information processing systems*, 2008.
- [31] Aviral Kumar, Justin Fu, Matthew Soh, George Tucker, and Sergey Levine. Stabilizing off-policy q-learning via bootstrapping error reduction. In *Advances in Neural Information Processing Systems*, 2019.
- [32] Arsenii Kuznetsov, Pavel Shvechikov, Alexander Grishin, and Dmitry Vetrov. Controlling overestimation bias with truncated mixture of continuous distributional quantile critics. In *International Conference on Machine Learning*, 2020.
- [33] Alex X. Lee, Anusha Nagabandi, Pieter Abbeel, and Sergey Levine. Stochastic latent actor-critic: Deep reinforcement learning with a latent variable model. In *Advances in Neural Information Processing Systems*, 2020.
- [34] Sergey Levine. Reinforcement Learning and Control as Probabilistic Inference: Tutorial and review. *arXiv preprint arXiv:1805.00909*, 2018.
- [35] Sergey Levine, Aviral Kumar, George Tucker, and Justin Fu. Offline reinforcement learning: Tutorial, review, and perspectives on open problems. *arXiv preprint arXiv:2005.01643*, 2020.
- [36] Timothy P. Lillicrap, Jonathan J. Hunt, Alexander Pritzel, Nicolas Heess, Tom Erez, Yuval Tassa, David Silver, and Daan Wierstra. Continuous control with deep reinforcement learning. In *International Conference on Learning Representations*, 2016.
- [37] Hao Liu, Yihao Feng, Yi Mao, Dengyong Zhou, Jian Peng, and Qiang Liu. Action-depedent control variates for policy optimization via stein’s identity. *arXiv preprint arXiv:1710.11198*, 2017.
- [38] Qiang Liu and Dilin Wang. Stein variational gradient descent: A general purpose bayesian inference algorithm. *arXiv preprint arXiv:1608.04471*, 2016.
- [39] Volodymyr Mnih, Koray Kavukcuoglu, David Silver, Alex Graves, Ioannis Antonoglou, Daan Wierstra, and Martin Riedmiller. Playing atari with deep reinforcement learning. *arXiv preprint arXiv:1312.5602*, 2013.

- [40] Rémi Munos, Tom Stepleton, Anna Harutyunyan, and Marc G. Bellemare. Safe and efficient off-policy reinforcement learning. In *Advances in Neural Information Processing Systems*, 2016.
- [41] Ofir Nachum, Mohammad Norouzi, and Dale Schuurmans. Improving policy gradient by exploring under-appreciated rewards. In *International Conference on Learning Representations*, 2017.
- [42] Ashvin Nair, Murtaza Dalal, Abhishek Gupta, and Sergey Levine. Accelerating online reinforcement learning with offline datasets. *arXiv preprint arXiv:2006.09359*, 2020.
- [43] Gerhard Neumann et al. Variational inference for policy search in changing situations. In *International Conference on Machine Learning*, 2011.
- [44] Mohammad Norouzi, Samy Bengio, Navdeep Jaitly, Mike Schuster, Yonghui Wu, Dale Schuurmans, et al. Reward augmented maximum likelihood for neural structured prediction. In *Advances In Neural Information Processing Systems*, 2016.
- [45] Brendan O’Donoghue, Ian Osband, and Catalin Ionescu. Making sense of reinforcement learning and probabilistic inference. In *International Conference on Learning Representations*, 2020.
- [46] Junhyuk Oh, Yijie Guo, Satinder Singh, and Honglak Lee. Self-imitation learning. In *International Conference on Machine Learning*, 2018.
- [47] Masashi Okada and Tadahiro Taniguchi. Variational inference mpc for bayesian model-based reinforcement learning. In *Conference on Robot Learning*, 2019.
- [48] Xue Bin Peng, Aviral Kumar, Grace Zhang, and Sergey Levine. Advantage-Weighted Regression: Simple and scalable off-policy reinforcement learning. *arXiv preprint arXiv:1910.00177*, 2019.
- [49] Jan Peters and Stefan Schaal. Reinforcement learning by reward-weighted regression for operational space control. In *Proceedings of the 24th international conference on Machine learning*, 2007.
- [50] Jan Peters, Katharina Mülling, and Yasemin Altın. Relative entropy policy search. In *AAAI Conference on Artificial Intelligence*, 2010.
- [51] Konrad Rawlik, Marc Toussaint, and Sethu Vijayakumar. On stochastic optimal control and reinforcement learning by approximate inference. In *International Joint Conference on Artificial Intelligence*, 2012.
- [52] John Schulman, Sergey Levine, Philipp Moritz, Michael Jordan, and Pieter Abbeel. Trust region policy optimization. In *International Conference on Machine Learning*, 2015.
- [53] John Schulman, Philipp Moritz, Sergey Levine, Michael Jordan, and Pieter Abbeel. High-dimensional continuous control using generalized advantage estimation. In *International Conference on Learning Representations*, 2016.
- [54] John Schulman, Filip Wolski, Prafulla Dhariwal, Alec Radford, and Oleg Klimov. Proximal policy optimization algorithms. *arXiv preprint arXiv:1707.06347*, 2017.
- [55] Noah Y. Siegel, Jost Tobias Springenberg, Felix Berkenkamp, Abbas Abdolmaleki, Michael Neunert, Thomas Lampe, Roland Hafner, and Martin A. Riedmiller. Keep doing what worked: Behavioral modelling priors for offline reinforcement learning. In *International Conference on Learning Representations*, 2020.
- [56] H. Francis Song, Abbas Abdolmaleki, Jost Tobias Springenberg, Aidan Clark, Hubert Soyer, Jack W. Rae, Seb Noury, Arun Ahuja, Siqi Liu, Dhruva Tirumala, Nicolas Heess, Dan Belov, Martin Riedmiller, and Matthew M. Botvinick. V-mpo: On-policy maximum a posteriori policy optimization for discrete and continuous control. In *International Conference on Learning Representations*, 2020.
- [57] Yunhao Tang and Alp Kucukelbir. Hindsight expectation maximization for goal-conditioned reinforcement learning. *arXiv preprint arXiv:2006.07549*, 2020.
- [58] Yuval Tassa, Yotam Doron, Alistair Muldal, Tom Erez, Yazhe Li, Diego de Las Casas, David Budden, Abbas Abdolmaleki, Josh Merel, Andrew Lefrancq, Timothy Lillicrap, and Martin Riedmiller. Deepmind control suite. *arXiv preprint arXiv:1801.00690*, 2018.
- [59] Emanuel Todorov. Linearly-solvable markov decision problems. In *Advances in Neural Information Processing Systems*, 2006.
- [60] Emanuel Todorov. General duality between optimal control and estimation. In *IEEE Conference on Decision and Control*, 2008.

- [61] Marc Toussaint. Robot trajectory optimization using approximate inference. In *International Conference on Machine Learning*, 2009.
- [62] Marc Toussaint and Amos Storkey. Probabilistic inference for solving discrete and continuous state markov decision processes. In *International conference on Machine learning*, 2006.
- [63] George Tucker, Surya Bhupatiraju, Shixiang Gu, Richard Turner, Zoubin Ghahramani, and Sergey Levine. The mirage of action-dependent baselines in reinforcement learning. In *International Conference on Machine Learning*, 2018.
- [64] Nino Vieillard, Tadashi Kozuno, Bruno Scherrer, Olivier Pietquin, Rémi Munos, and Matthieu Geist. Leverage the average: an analysis of kl regularization in rl. In *Advances in Neural Information Processing Systems*, 2021.
- [65] Tingwu Wang, Xuchan Bao, Ignasi Clavera, Jerrick Hoang, Yeming Wen, Eric Langlois, Shunshi Zhang, Guodong Zhang, Pieter Abbeel, and Jimmy Ba. Benchmarking model-based reinforcement learning. *arXiv preprint arXiv:1907.02057*, 2019.
- [66] Ziyu Wang, Alexander Novikov, Konrad Zolna, Jost Tobias Springenberg, Scott Reed, Bobak Shahriari, Noah Siegel, Josh Merel, Caglar Gulcehre, Nicolas Heess, and Nando de Freitas. Critic regularized regression. *arXiv preprint arXiv:2006.15134*, 2020.
- [67] Cathy Wu, Aravind Rajeswaran, Yan Duan, Vikash Kumar, Alexandre M Bayen, Sham Kakade, Igor Mordatch, and Pieter Abbeel. Variance reduction for policy gradient with action-dependent factorized baselines. *arXiv preprint arXiv:1803.07246*, 2018.
- [68] Yifan Wu, George Tucker, and Ofir Nachum. Behavior Regularized Offline Reinforcement Learning. *arXiv preprint arXiv:1911.11361*, 2019.

## Checklist

1. For all authors...
  - (a) Do the main claims made in the abstract and introduction accurately reflect the paper’s contributions and scope? **[Yes]**
  - (b) Did you describe the limitations of your work? **[Yes]** We added the failure cases of ablations that end up the insufficient coverage and the unclear insights in Appendix H.
  - (c) Did you discuss any potential negative societal impacts of your work? **[Yes]** Actually, we conducted exhaustive evaluations through the enormous experiments, which might lead to force the future research to spend much computing resources. We hope our empirical observations and recommendations help the practitioners to explore the explosive configuration space.
  - (d) Have you read the ethics review guidelines and ensured that your paper conforms to them? **[Yes]**
2. If you are including theoretical results...
  - (a) Did you state the full set of assumptions of all theoretical results? **[N/A]**
  - (b) Did you include complete proofs of all theoretical results? **[N/A]**
3. If you ran experiments...
  - (a) Did you include the code, data, and instructions needed to reproduce the main experimental results (either in the supplemental material or as a URL)? **[Yes]** We open-source the codebase at <https://github.com/frt03/inference-based-rl>.
  - (b) Did you specify all the training details (e.g., data splits, hyperparameters, how they were chosen)? **[Yes]** See Appendix A.
  - (c) Did you report error bars (e.g., with respect to the random seed after running experiments multiple times)? **[Yes]** Our experimental results were averaged among 10 random seeds.
  - (d) Did you include the total amount of compute and the type of resources used (e.g., type of GPUs, internal cluster, or cloud provider)? **[Yes]** See Appendix A.
4. If you are using existing assets (e.g., code, data, models) or curating/releasing new assets...
  - (a) If your work uses existing assets, did you cite the creators? **[Yes]** We cited the authors of the codebase in Sec. 4.3.
  - (b) Did you mention the license of the assets?
  - (c) Did you include any new assets either in the supplemental material or as a URL? **[N/A]**
  - (d) Did you discuss whether and how consent was obtained from people whose data you’re using/curating? **[N/A]**

- (e) Did you discuss whether the data you are using/curating contains personally identifiable information or offensive content? [N/A]
5. If you used crowdsourcing or conducted research with human subjects...
- (a) Did you include the full text of instructions given to participants and screenshots, if applicable? [N/A]
  - (b) Did you describe any potential participant risks, with links to Institutional Review Board (IRB) approvals, if applicable? [N/A]
  - (c) Did you include the estimated hourly wage paid to participants and the total amount spent on participant compensation? [N/A]

## Appendix

### A Network Architectures

In this section, we describe the details of the network architectures used in Sec. 4 and 5.

We mainly used 4 GPUs (NVIDIA V100; 16GB) for the experiments in Sec. 4 and 5 and it took about 4 hours per seed (in the case of 3M steps). Actually, we conducted exhaustive evaluations through the enormous experiments, and we hope our empirical observations and recommendations help the practitioners to explore the explosive configuration space.

Architecture	MPO	AWR	AWAC	SAC
Policy network	(256, 256, 256)	(128, 64)	(256, 256)	(256, 256)
Value network	(512, 512, 256)	(128, 64)	(256, 256)	(256, 256)
Activation function	ELU	ReLU	ReLU	ReLU
Layer normalization	✓	–	–	–
Input normalization	–	✓	–	–
Optimizer	Adam	SGD (momentum=0.9)	Adam	Adam
Learning rate (policy)	1e-4	5e-5	3e-4	3e-4
Learning rate (value)	1e-4	1e-2	3e-4	3e-4
Weight initialization	Uniform	Xavier Uniform	Xavier Uniform	Xavier Uniform
Initial output scale (policy)	1.0	1e-4	1e-2	1e-2
Target update	Hard	–	Soft (5e-3)	Soft (5e-3)
Clipped Double Q	False	–	True	True

Table 7: Details of each network architecture. We refer the original implementations of each algorithm which is available online [23, 14, 48, 27, 42]. Note that AWR uses different learning rates of the policy per environment.

MPO	Hopper-v2	Walker2d-v2	HalfCheetah-v2	Ant-v2	Humanoid-v2	Swimmer-v2
Learning rate ( $\eta$ )	1e-2					
Dual constraint	1e-1					
Mean constraint	3.34e-4	1.67e-4	1e-3	1e-3	5.88e-5	1e-3
Stddev constraint	3.34e-7	1.67e-7	1e-6	1e-6	5.88e-8	1e-6
Action penalty constraint	1e-3					
Initial stddev scale	0.7	0.3	0.5	0.5	0.3	0.5
Discount factor $\gamma$	0.99					

Table 8: Hyper-parameters of MPO. We follow the implementation by Hoffman et al. [27]. Some of mean & stddev constraint are divided by the number of dimensions in the action space as suggested by Hoffman et al. [27], which is empirically better.

AWR	Hopper-v2	Walker2d-v2	HalfCheetah-v2	Ant-v2	Humanoid-v2	Swimmer-v2
Learning rate (policy)	1e-4	2.5e-5	5e-5	5e-5	1e-5	5e-5
Stddev scale	0.4	0.4	0.4	0.2	0.4	0.4
Exp-Advantage Weight clip	20.0					
Action penalty coefficient	10.0					
Discount factor $\gamma$	0.99					
$\lambda$ for TD( $\lambda$ )	0.95					

Table 9: Hyper-parameters of AWR. We follow the implementation by Peng et al. [48].

**Small Network (AWR)** We denote the policy and value network used in AWR as a small (S) network, described as follows (in Sec. 5.4, we didn’t change the activation and distribution):

```

from torch import nn

activation = nn.ReLU()
distribution = GaussianHeadWithFixedCovariance()

policy = nn.Sequential(
    nn.Linear(obs_size, 128),

```



```

        activation,
        nn.Linear(128, 64),
        activation,
        nn.Linear(64, action_size),
        distribution,
    )
    vf = nn.Sequential(
        nn.Linear(obs_size, 128),
        activation,
        nn.Linear(128, 64),
        activation,
        nn.Linear(64, 1),
    )

```

**Medium Network (SAC)** We denote the policy and value network used in SAC as a medium (M) network, described as follows (in Sec. 5.4, we didn't change the activation and distribution):

```

from torch import nn

activation = nn.ReLU()
distribution = TanhSquashedDiagonalGaussian()

policy = nn.Sequential(
    nn.Linear(obs_size, 256),
    activation,
    nn.Linear(256, 256),
    activation,
    nn.Linear(256, action_size * 2),
    distribution
)
q_func = nn.Sequential(
    ConcatObsAndAction(),
    nn.Linear(obs_size + action_size, 256),
    activation,
    nn.Linear(256, 256),
    activation,
    nn.Linear(256, 1)
)

```

**Large Network (MPO)** We denote the policy and value network used in MPO as a large (L) network, described as follows (in Sec. 5.4, we didn't change the activation and distribution):

```

from torch import nn

activation = nn.ELU()
distribution = GaussianHeadWithDiagonalCovariance()

policy = nn.Sequential(
    nn.Linear(obs_size, 256),
    nn.LayerNorm(256),
    nn.Tanh(),
    activation,
    nn.Linear(256, 256),
    activation,
    nn.Linear(256, 256),
    activation,
    nn.Linear(256, action_size * 2),
    distribution
)
q_func = nn.Sequential(
    ConcatObsAndAction(),
    nn.Linear(obs_size + action_size, 512),
    nn.LayerNorm(512),
    nn.Tanh(),
    activation,

```

```

    nn.Linear(512, 512),
    activation,
    nn.Linear(512, 256),
    activation,
    nn.Linear(256, 1)
)

```

## B Relations to Other Algorithms

We here explain the relation of the unified policy iteration scheme covers other algorithms. While we mainly focused on AWR, MPO, and SAC in the this paper, our unified scheme covers other algorithms too, as summarized in Table 1:

### EM control algorithms:

- PoWER [30]:  $\pi_p (= \pi_\theta)$  update is analytic.  $\mathcal{G} = \eta \log Q^{\pi_p}$  and  $Q^{\pi_p}$  is estimated by TD(1).  $\pi_\theta = \mathcal{N}(\mu_\theta(s), \Sigma_\theta(s))$ .
- RWR [49]:  $\pi_p = \pi_\theta$  is updated by SG.  $\mathcal{G} = \eta \log r$ , and  $\pi_\theta = \mathcal{N}(\mu_\theta(s), \Sigma)$ . When the reward is unbounded, RWR requires adaptive reward transformation (e.g.  $u_\beta(r(s, a)) = \beta \exp(-\beta r(s, a))$ );  $\beta$  is a learnable parameter).
- REPS [50]:  $\pi_p$  is  $\pi_q$  of the previous EM step (on-policy) or a mixture of all previous  $\pi_q$  (off-policy), which is approximated by samples.  $\mathcal{G} = A^{\pi_p}$  and estimated by a single-step TD error with a state-value function computed by solving a dual function.  $\pi_q$  is assumed as a softmax policy for discrete control in the original paper.
- UREX [41]:  $\pi_p = \pi_\theta$  is updated by SG.  $\mathcal{G} = Q^{\pi_p}$  and estimated by TD(1).  $\pi_\theta$  is assumed as a softmax policy for discrete control in the original paper.
- V-MPO [56]: Almost the same as MPO, but a state-value function is trained by  $n$ -step bootstrap instead of Q-function. Top-K advantages are used in E-step.

### KL control algorithms:

- TRPO [52]:  $\pi_q = \pi_\theta = \mathcal{N}(\mu_\theta(s), \Sigma_\theta)$ . The KL penalty is converted to a constraint, and the direction of the KL is reversed.  $\mathcal{G} = A^{\pi_p}$  and estimated by TD(1).  $\pi_p$  is continuously updated to  $\pi_q$ .
- PPO with a KL penalty [54]:  $\pi_q = \pi_\theta = \mathcal{N}(\mu_\theta(s), \Sigma_\theta)$ . The direction of the KL penalty is reversed.  $\mathcal{G} = A^{\pi_p}$  and estimated by GAE [53]. An adaptive  $\eta$  is used so that  $D_{KL}(\pi_p || \pi_q)$  approximately matches to a target value.
- DDPG<sup>3</sup> [36]:  $\pi_q = \pi_\theta$  is the delta distribution and updated by SG.  $\mathcal{G} = Q^{\pi_q}$  and estimated by TD(0).  $\eta = 0$  (i.e., the KL divergence and  $\pi_p$  update are ignored).
- TD3<sup>2</sup> [13]: It is a variant of DDPG and leverages three implementational techniques, clipped double Q-learning, delayed policy updates, and target policy smoothing.
- BRAC [68] and BEAR [31] (Offline RL): When we assume  $\pi_p = \pi_b$  (any behavior policy), and omitting its update, some of the offline RL methods, such as BRAC or BEAR, can be interpreted as one of the KL control methods. Both algorithms utilize the variants of clipped double Q-learning ( $\lambda$ -interpolation between max and min).

---

<sup>3</sup>Note that DDPG and TD3 are not the “inference-based” algorithms, but we can classify these two as KL control variants.

## C Benchmarks on DeepMind Control Suite

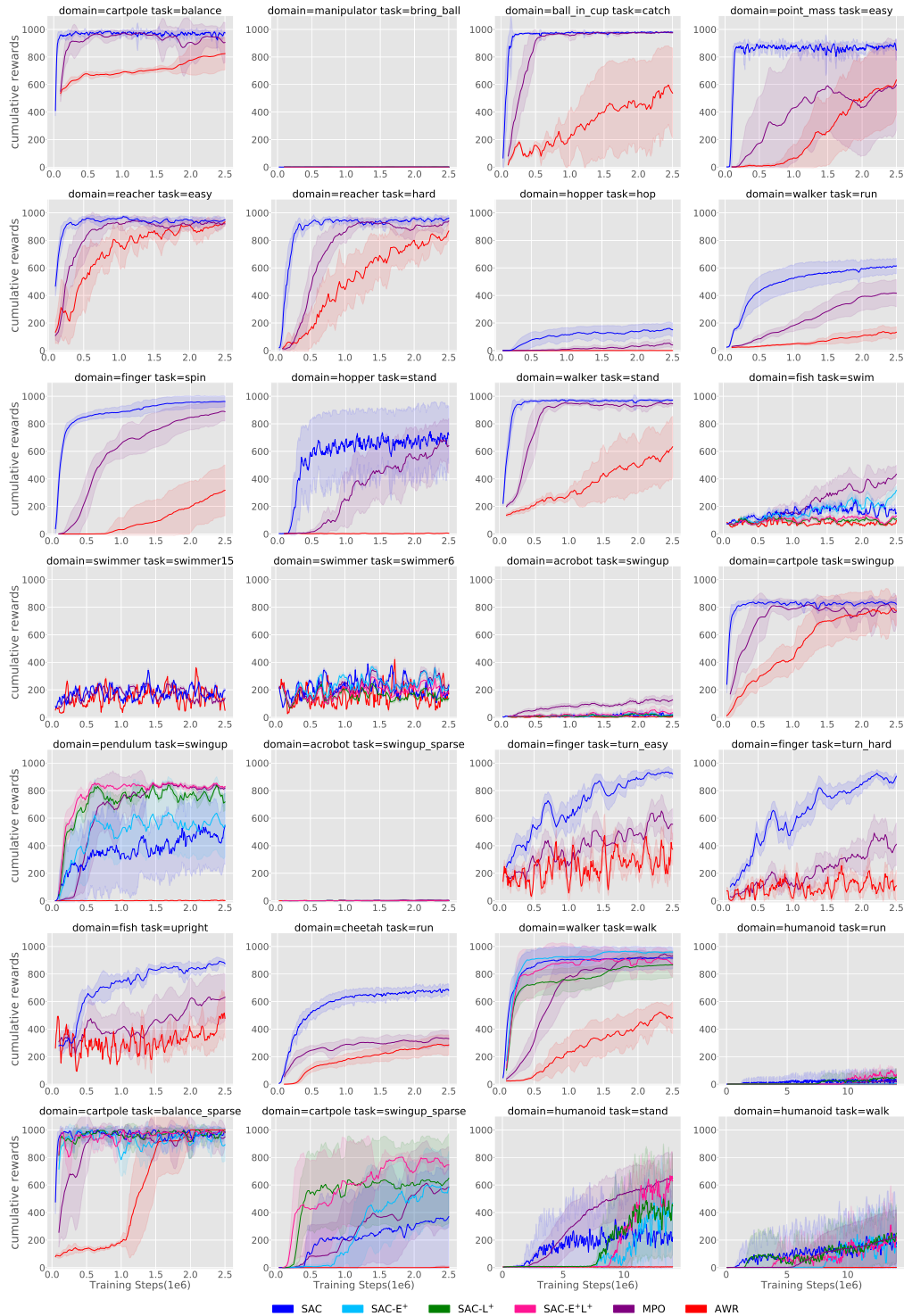


Figure 2: Benchmarking results on DeepMind Control Suite 28 environments. The performances are averaged among 10 random seeds. We use an action repeat of 1 throughout all experiments for simplicity.

In this section, we show the benchmarking results on 28 tasks in DeepMind Control Suite (Figure 2). Each algorithm is run with 2.5M steps (except for humanoid domain; 14M steps), following Abdolmaleki et al. [2]. While the previous work mentioned that tuning the number of action repeats was effective [33], we used an action repeat of 1 throughout all experiments for simplicity. We also use the hyper-parameters of each algorithm

presented in Appendix A. As discussed in Sec. 5.3, we incorporate ELU and layer normalization into SAC in several domains where SAC is behind MPO or AWR. ELU and layer normalization significantly improve performances, especially in pendulum\_swingup and cartpole\_swingup\_sparse. Some of MPO results don't seem to match the original paper, but we appropriately confirmed that these results are equivalent to those of its public implementation [27].

	SAC	SAC-E <sup>+</sup>	SAC-L <sup>+</sup>	SAC-E <sup>+</sup> L <sup>+</sup>	MPO	AWR
cartpole_balance	<b>975 ± 12</b>	–	–	–	824 ± 118	905 ± 146
manipulator_bring_ball	0.27 ± 0.0	0.80 ± 0.1	<b>0.96 ± 0.3</b>	0.72 ± 0.1	0.79 ± 0.1	0.85 ± 0.2
ball_in_cup_catch	<b>980 ± 0.5</b>	–	–	–	976 ± 6	538 ± 328
point_mass_easy	<b>850 ± 75</b>	–	–	–	632 ± 254	597 ± 329
reacher_easy	<b>949 ± 14</b>	–	–	–	920 ± 18	934 ± 25
reacher_hard	<b>962 ± 18</b>	–	–	–	941 ± 22	868 ± 70
hopper_hop	<b>151 ± 50</b>	–	–	–	41 ± 22	0.1 ± 0.2
walker_run	<b>615 ± 56</b>	–	–	–	416 ± 99	133 ± 40
finger_spin	<b>962 ± 39</b>	–	–	–	888 ± 69	317 ± 185
hopper_stand	<b>720 ± 207</b>	–	–	–	640 ± 199	5 ± 1
walker_stand	<b>972 ± 6</b>	–	–	–	945 ± 18	633 ± 221
fish_swim	152 ± 23	317 ± 32	108 ± 9	130 ± 6	<b>434 ± 66</b>	97 ± 13
swimmer_swimmer15	<b>199 ± 15</b>	–	–	–	139 ± 14	52 ± 4
swimmer_swimmer6	229 ± 12	223 ± 11	138 ± 13	189 ± 17	<b>238 ± 29</b>	170 ± 4
acrobot_swingup	10 ± 10	21 ± 10	15 ± 7	34 ± 27	<b>127 ± 36</b>	4 ± 2
cartpole_swingup	<b>822 ± 45</b>	–	–	–	776 ± 109	767 ± 106
pendulum_swingup	542 ± 279	550 ± 232	718 ± 62	<b>830 ± 4</b>	819 ± 11	1 ± 4
acrobot_swingup_sparse	0.40 ± 0.1	0.43 ± 0.2	0.46 ± 0.0	0.42 ± 0.1	<b>4 ± 4</b>	0.0 ± 0.0
finger_turn_easy	<b>922 ± 34</b>	–	–	–	556 ± 116	374 ± 117
finger_turn_hard	<b>904 ± 21</b>	–	–	–	410 ± 156	109 ± 113
fish_upright	<b>876 ± 25</b>	–	–	–	631 ± 166	478 ± 143
cheetah_run	<b>682 ± 44</b>	–	–	–	331 ± 60	285 ± 73
walker_walk	916 ± 77	<b>960 ± 7</b>	866 ± 93	875 ± 97	931 ± 25	482 ± 115
humanoid_run	17 ± 47	3 ± 2	52 ± 62	<b>71 ± 39</b>	22 ± 42	0.8 ± 0.0
cartpole_balance_sparse	987 ± 27	892 ± 119	982 ± 30	982 ± 10	949 ± 76	<b>1000 ± 0.0</b>
cartpole_swingup_sparse	370 ± 370	582 ± 261	648 ± 324	<b>745 ± 36</b>	585 ± 294	3 ± 10
humanoid_stand	221 ± 231	469 ± 245	448 ± 359	630 ± 129	<b>651 ± 183</b>	6 ± 0.0
humanoid_walk	182 ± 255	166 ± 148	<b>250 ± 209</b>	219 ± 177	224 ± 197	1 ± 0.0

Table 10: Raw scores of Figure 2. The performances are averaged among 10 random seeds. Each algorithm is run with 2.5M steps (except for humanoid domain; 14M steps), following Abdolmaleki et al. [2]. We use an action repeat of 1 throughout all experiments for simplicity.

## D Benchmarks on MuJoCo Manipulation Tasks

We extensively evaluate their performance in the manipulation tasks (Figure 3). The trend seems the same as the locomotion tasks, while AWR beats SAC and MPO in Striker, which means they fall into sub-optimal.

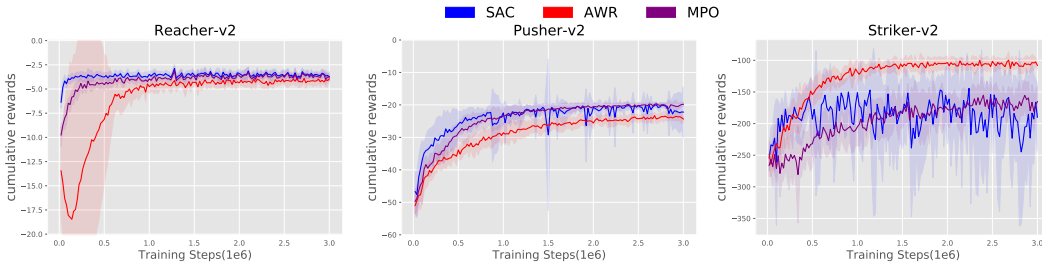


Figure 3: Benchmarking results on OpenAI Gym MuJoCo manipulation environments. All experiments are run with 10 random seeds. SAC and MPO completely solve Reacher and Pusher, while in Striker they fall into sub-optimal.

## E Reproduction Results of AWR on MuJoCo Locomotion Environments

We re-implemented AWR based on PFRL, a pytorch-based RL library [14], referring its original implementation [48]. Figure 4 shows the performance of our implementation in the original experimental settings, also following hyper-parameters. We recovered the original results in Peng et al. [48] properly.

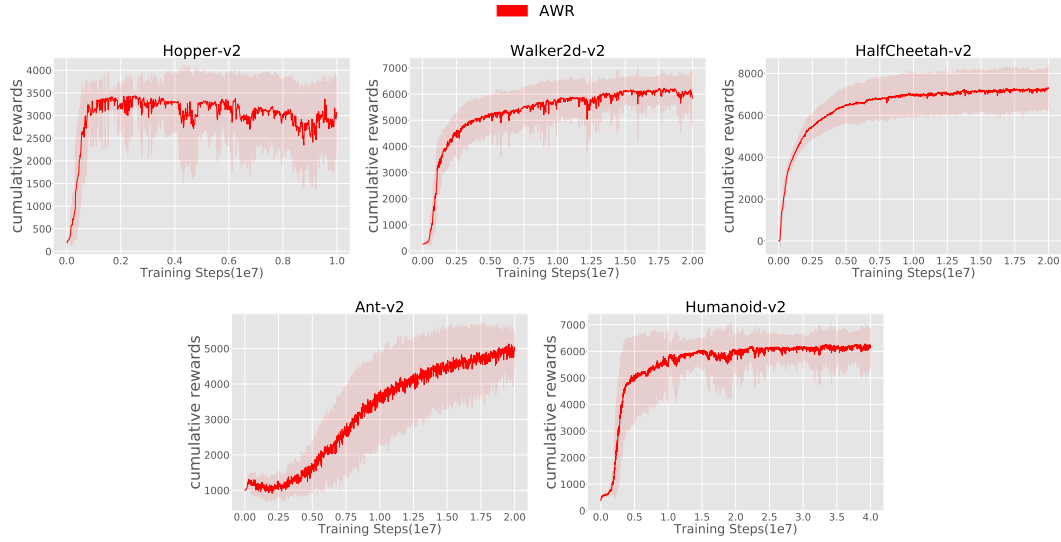


Figure 4: Reproduction of Advantage Weighted Regression (AWR). We obtained comparable results to the original paper.

## F Learning Curves

In this section, we present learning curves of the experiments in Sec. 5.

### F.1 Clipped Double Q-Learning

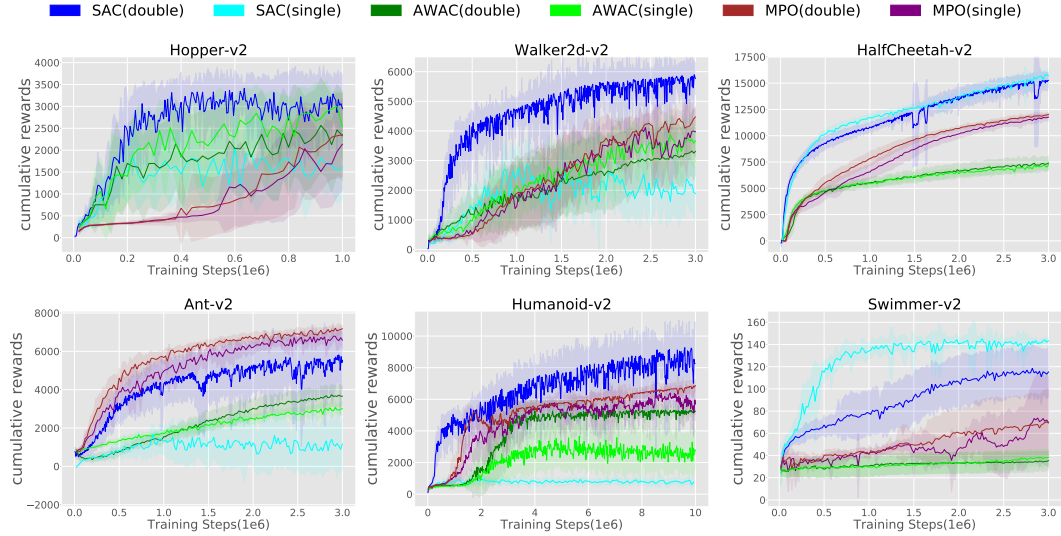


Figure 5: The learning curves of Table 2; ablation of Clipped Double Q-Learning. We test original SAC (double), AWAC (double), MPO (single), and some variants; SAC without clipped double Q-learning (single), AWAC (single), and MPO with clipped double Q-learning (double).

### F.2 Action Distribution for the Policy

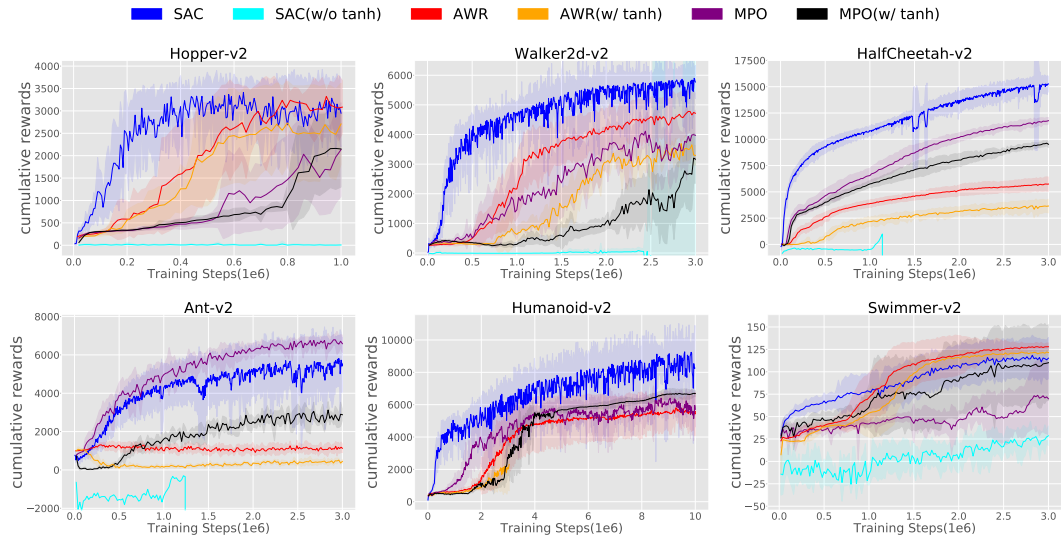


Figure 6: The learning curves of Table 3; ablation of Tanh transformation. A line that stopped in the middle means that its training has stopped at that step due to numerical error. We test SAC without tanh squashing, AWR with tanh, and MPO with tanh.

### F.3 Activation and Normalization

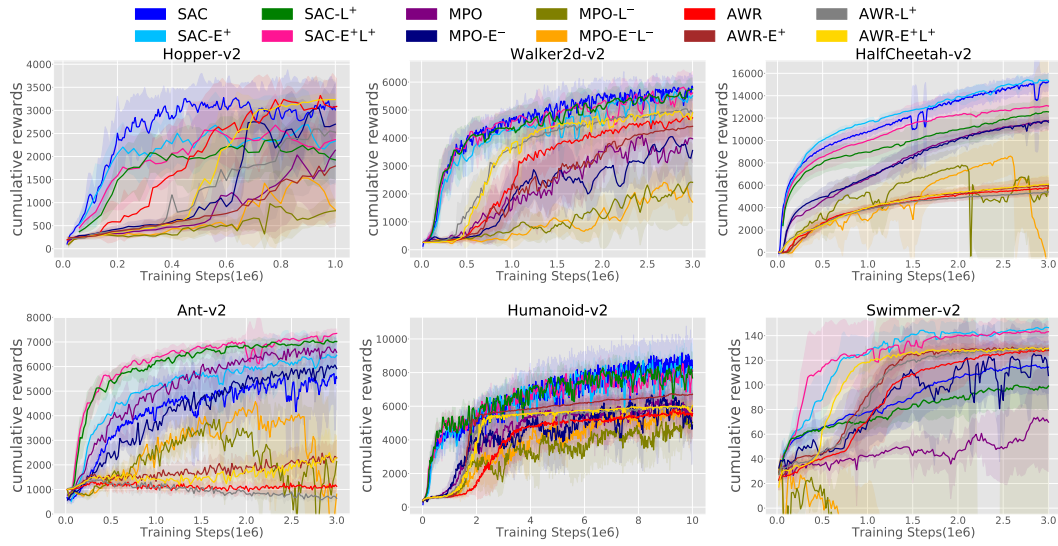


Figure 7: The learning curves of Table 4; incorporating ELU/layer normalization into SAC and AWR.  $E^+/L^+$  indicates adding, and  $E^-/L^-$  indicates removing ELU/layer normalization.

### F.4 Network Size

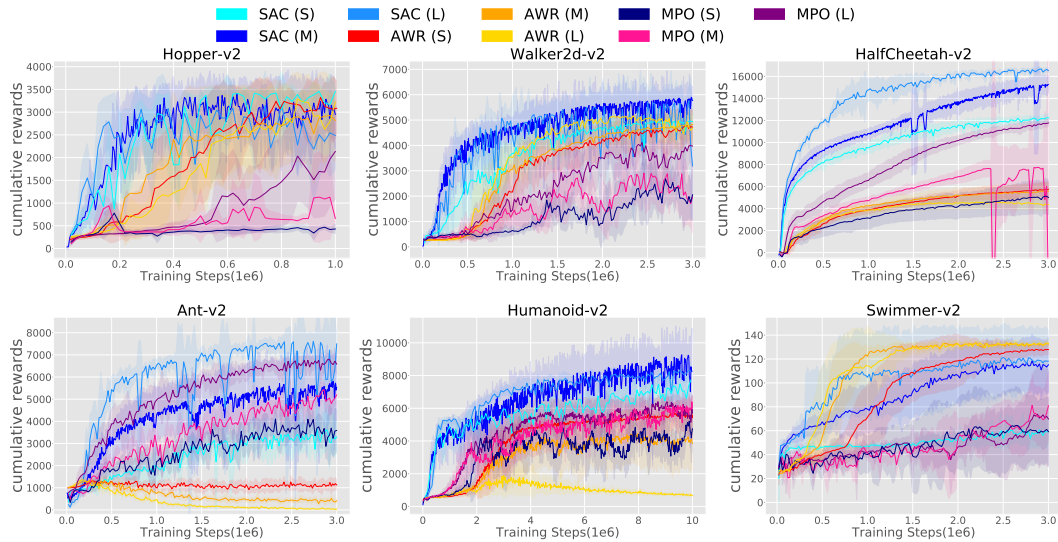


Figure 8: The learning curves of Table 5; experiment for finer network sizes. (S) stands for the small network size from AWR, (M) for the middle network size from SAC, and (L) for the large network size from MPO.

## G Additional Experiments for Deeper Analysis of Implementation Details

We share the additional experimental results for deeper analysis of implementation details and co-adaptation nature. We report the final cumulative return after 3M steps for Ant/HalfCheetah/Walker2d/Swimmer, 1M steps for Hopper, and 10M steps for Humanoid. All results below are averaged among 10 random seeds. These extensive experimental observations below suggest not only the co-adaptive nature and transferability of each implementation and code detail (discussed in Sec. 6), but also the properties of each kind of algorithm (KL-based and EM-based); **KL-based methods, such as SAC, shows the co-dependent nature in implementation details (clipped double Q-learning, Tanh-Gaussian Policy) but robustness to the code details related to neural networks. In contrast, EM-based methods, such as MPO and AWR, show the co-dependent nature in code details but robustness to the implementation details.** We hope these empirical observations from our experiments are valuable contributions to the RL community.

$\pi_p$  **Update** We test different types of  $\pi_p$  Update as summarized in Table 1 to investigate the effectiveness of implementation choices. We prepare 4 variants: (1) MPO or AWAC with a uniform prior, (2) SAC with target policy instead of a fixed uniform prior, (3) MPO without trust-region (only SG update). The details of (1) - (3) are described below:

- (1) We use the actions sampled from uniform distribution as well as the samples from the policy at the past iteration  $\pi_{\theta_p^{(k-1)}}$  for the M-step in EM-controls;  $a_j \sim \alpha \text{Unif.} + (1 - \alpha)\pi_{\theta_p^{(k-1)}}$ ,  $\alpha \in (0, 1]$ . These variants are much closer to SAC (using uniform distribution as  $\pi_p$ ). We test  $\alpha = 0.25, 0.5, 0.75$  for both MPO and AWAC.
- (2) We copy the parameter of  $\pi_q$  at a certain interval and use it as  $\pi_p$  in the objective of KL Control, similar to MPO/PPO/TRPO. It seems “KL-regularized” actor-critic, rather than “soft” (entropy-regularized). We test both Lagrangian constraint ( $\epsilon = 0.1, 0.01, 0.001$ ) and regularization coefficient ( $\eta = 1.0, 0.1, 0.01$ ).
- (3) Original MPO stabilizes the  $\pi_p$  Update incorporating TR (trust-region) into SG. We test the effect of TR, just removing TR term in the M-step of MPO.

However, the variants listed above have shown drastic degradation compared to the original choice (we omit the performance table since most of them failed). For example, the larger  $\alpha$  (1) we chose, the lower scores the algorithm achieved. Also, KL-SAC (2) did not learn meaningful behaviors, and removing TR from MPO (3) induced significant performance drops. These failures suggest that the implementation choice of  $\pi_p$  Update might be the most important one and should be designed carefully for both KL and EM control families.

$\mathcal{G}$ : **Soft Q-function** We investigate the effect of the soft Q-function, instead of standard Q function as MPO or AWAC use. We prepare MPO with soft Q, AWAC with soft Q, and SAC without soft Q-function, just modifying Bellman equation and keep the policy objectives as they are.

Table 11 shows that SAC without soft Q degrades its performance over 5 tasks except for Ant, while it is not so drastic compared to clipped double Q or Tanh-Gaussian policy. In contrast, MPO with soft Q slightly improves the performance (over 4 tasks), and AWAC with soft Q slightly also does (over 3 tasks). These trends are similar to the clipped double Q or Tanh-Gaussian policy. We think these experiments support our empirical observation: KL-based methods, such as SAC, show the robustness to the code details, while EM-based methods, such as MPO and AWR, show the co-dependent nature in code details but robustness to the implementation details.

	Hopper-v2	Walker2d-v2	HalfCheetah-v2	Ant-v2	Humanoid-v2	Swimmer-v2
<b>SAC</b>	<b>3013 ± 602</b>	<b>5820 ± 411</b>	<b>15254 ± 751</b>	5532 ± 1266	<b>8081 ± 1149</b>	<b>114 ± 21</b>
<b>SAC (w/o Soft Q)</b>	2487 ± 870	5674 ± 202	12319 ± 2731	6496 ± 305	6772 ± 3060	<b>114 ± 33</b>
<b>MPO</b>	2136 ± 1047	3972 ± 849	11769 ± 321	<b>6584 ± 455</b>	5709 ± 1081	70 ± 40
<b>MPO (w/ Soft Q)</b>	2271 ± 1267	3817 ± 794	11911 ± 274	6312 ± 332	6571 ± 461	80 ± 32
<b>AWAC</b>	2329 ± 1020	3307 ± 780	7396 ± 677	3659 ± 523	5243 ± 200	35 ± 8
<b>AWAC (w/ Soft Q)</b>	2545 ± 1062	3671 ± 575	7199 ± 628	3862 ± 483	5152 ± 162	35 ± 10

Table 11: Ablation of Soft Q-function (the choice of  $\mathcal{G}$  in Table 1), adding to MPO and AWAC while removing from SAC.

**Network Size for AWAC** To investigate the co-dependent nature between implementation and code details more precisely, we add the network size ablation of AWAC, whose implementations stand between MPO and AWR. AWAC differs  $\pi_p$  Update and network size (the default choice of AWAC is (M)) from MPO (in fact, MPO uses TD(0) in open-source implementation [27] and we assume the difference of  $\pi_\theta$  might be minor). Also, AWAC differs  $\mathcal{G}$  and  $\mathcal{G}$  estimate from AWR.

The results of AWAC (Table 12) show a similar trend to AWR in high-dimensional tasks (Ant, Humanoid); a larger network did not help. We may hypothesize that  $\pi_p$  Update of AWR/AWAC, mixture+SG, is not good at optimizing larger networks, compared to SG + TR of MPO. In contrast, especially, Hopper and Walker2d show a



similar trend to MPO; the larger, the better. Totally, AWAC with different network sizes shows the mixture trend of AWR and MPO, which is the same as implementation details. We think these observations might highlight the co-adaptation nature between implementation and code details.

	Hopper-v2	Walker2d-v2	HalfCheetah-v2	Ant-v2	Humanoid-v2	Swimmer-v2
<b>AWAC (L)</b>	<b>2764 ± 919</b>	<b>4350 ± 542</b>	6433 ± 832	2342 ± 269	4164 ± 1707	<b>40 ± 5</b>
<b>AWAC (M)</b>	2329 ± 1020	3307 ± 780	<b>7396 ± 677</b>	3659 ± 523	5243 ± 200	35 ± 8
<b>AWAC (S)</b>	2038 ± 1152	2022 ± 971	5864 ± 768	<b>3705 ± 659</b>	<b>5331 ± 125</b>	34 ± 11

Table 12: Ablation of network size for AWAC.

**Combination of Clipped Double Q-Learning/Tanh-Gaussian and Soft Q-function** We observe that both clipped double Q-learning/Tanh-Gaussian policy and soft Q-function are the important implementation choices to KL control, SAC, which lead to significant performance gains. To test the co-adaptation nature more in detail, we implement these two choices into MPO and AWAC at the same time.

The results (Table 13 and Table 14) show that incorporating such multiple combinations does not show any notable improvement in EM Controls, MPO and AWAC. They also suggest the co-adaptation nature of those two implementations to KL Controls, especially SAC.

	Hopper-v2	Walker2d-v2	HalfCheetah-v2	Ant-v2	Humanoid-v2	Swimmer-v2
<b>MPO (S)</b>	2136 ± 1047	3972 ± 849	11769 ± 321	6584 ± 455	5709 ± 1081	70 ± 40
<b>MPO (D)</b>	2352 ± 959	<b>4471 ± 281</b>	12028 ± 191	<b>7179 ± 190</b>	6858 ± 373	69 ± 29
<b>MPO (Soft Q, S)</b>	2271 ± 1267	3817 ± 794	11911 ± 274	6312 ± 332	6571 ± 461	<b>80 ± 32</b>
<b>MPO (Soft Q, D)</b>	1283 ± 632	4378 ± 252	<b>12117 ± 126</b>	6822 ± 94	<b>6895 ± 433</b>	45 ± 4
<b>AWAC (S)</b>	2540 ± 755	3662 ± 712	7226 ± 449	3008 ± 375	2738 ± 982	38 ± 7
<b>AWAC (D)</b>	2329 ± 1020	3307 ± 780	7396 ± 677	3659 ± 523	5243 ± 200	35 ± 8
<b>AWAC (Soft Q, S)</b>	<b>2732 ± 660</b>	3658 ± 416	7270 ± 185	3494 ± 330	2926 ± 1134	36 ± 10
<b>AWAC (Soft Q, D)</b>	2545 ± 1062	3671 ± 575	7199 ± 628	3862 ± 483	5152 ± 162	35 ± 10

Table 13: Ablation of combination in implementation components; Soft Q-function (the choice of  $\mathcal{G}$ ) and Clipped Double Q-Learning (the choice of  $\mathcal{G}$  estimate), adding to MPO and AWAC. (D) denotes algorithms with clipped double Q-learning, and (S) denotes without it.

	Hopper-v2	Walker2d-v2	HalfCheetah-v2	Ant-v2	Humanoid-v2	Swimmer-v2
<b>MPO</b>	2136 ± 1047	<b>3972 ± 849</b>	11769 ± 321	<b>6584 ± 455</b>	5709 ± 1081	70 ± 40
<b>MPO (Soft Q)</b>	2271 ± 1267	3817 ± 794	<b>11911 ± 274</b>	6312 ± 332	<b>6571 ± 461</b>	<b>80 ± 32</b>
<b>MPO (Soft Q, Tanh)</b>	314 ± 8 <sup>†</sup>	368 ± 47 <sup>†</sup>	3427 ± 207 <sup>†</sup>	628 ± 221 <sup>†</sup>	5919 ± 202 <sup>†</sup>	35 ± 8 <sup>†</sup>
<b>AWAC</b>	2329 ± 1020	3307 ± 780	7396 ± 677	3659 ± 523	5243 ± 200	35 ± 8
<b>AWAC (Soft Q)</b>	2545 ± 1062	3671 ± 575	7199 ± 628	3862 ± 483	5152 ± 162	35 ± 10
<b>AWAC (Soft Q, Tanh)</b>	<b>2989 ± 484</b>	2794 ± 1692	6263 ± 247	3507 ± 458	66 ± 4	32 ± 5

Table 14: Ablation of combination in implementation components; Soft Q-function (the choice of  $\mathcal{G}$ ) and Tanh-squashed Gaussian policy (the parameterization of the policy), adding to MPO and AWAC (<sup>†</sup>numerical error happens during training).

## H Failed Ablations

This section provides the failure case of ablations on tanh-squashed distributions and exchanging network architectures, which shows the catastrophic failure during training, and unclear insights.

### H.1 Action Distribution for the Policy: Without Action Clipping

We observe that naive application of tanh-squashing to MPO and AWR significantly suffers from numerical instability, which ends up with NaN outputs (Table 15 and Figure 9). As we point out in Sec. 5.2, the practical solution is to clip the action within the supports of distribution surely;  $a \in [-1 + \epsilon, 1 - \epsilon]^{|A|}$ .

```
eps = 1e-6
actions = torch.clamp(actions, min=-1.+eps, max=1.-eps)
```

	SAC (w/)	SAC (w/o)	AWR (w/)	AWR (w/o)	MPO (w/)	MPO (w/o)
Hopper-v2	3013 ± 602	6 ± 10	<b>3267 ± 383</b>	3085 ± 593	301 ± 12 <sup>†</sup>	2136 ± 1047
Walker2d-v2	<b>5820 ± 411</b>	−∞	3281 ± 1084 <sup>†</sup>	4717 ± 678	328 ± 95 <sup>†</sup>	3972 ± 849
HalfCheetah-v2	<b>15254 ± 751</b>	−∞	1159 ± 599 <sup>†</sup>	5742 ± 667	831 ± 242 <sup>†</sup>	11769 ± 321
Ant-v2	5532 ± 1266	−∞	152 ± 101 <sup>†</sup>	1127 ± 224	202 ± 102 <sup>†</sup>	<b>6584 ± 455</b>
Humanoid-v2	<b>8081 ± 1149</b>	108 ± 82 <sup>†</sup>	538 ± 49 <sup>†</sup>	5573 ± 1020	5642 ± 77 <sup>†</sup>	5709 ± 1081
Swimmer-v2	114 ± 21	28 ± 11	117 ± 16	<b>128 ± 4</b>	37 ± 6 <sup>†</sup>	70 ± 40

Table 15: Ablation of Tanh transformation (<sup>†</sup> numerical error happens during training). We test SAC without tanh squashing, AWR with tanh, and MPO with tanh. SAC without tanh transform results in drastic degradation of the performance, which can be caused by the maximum entropy objective that encourages the maximization of the covariance.

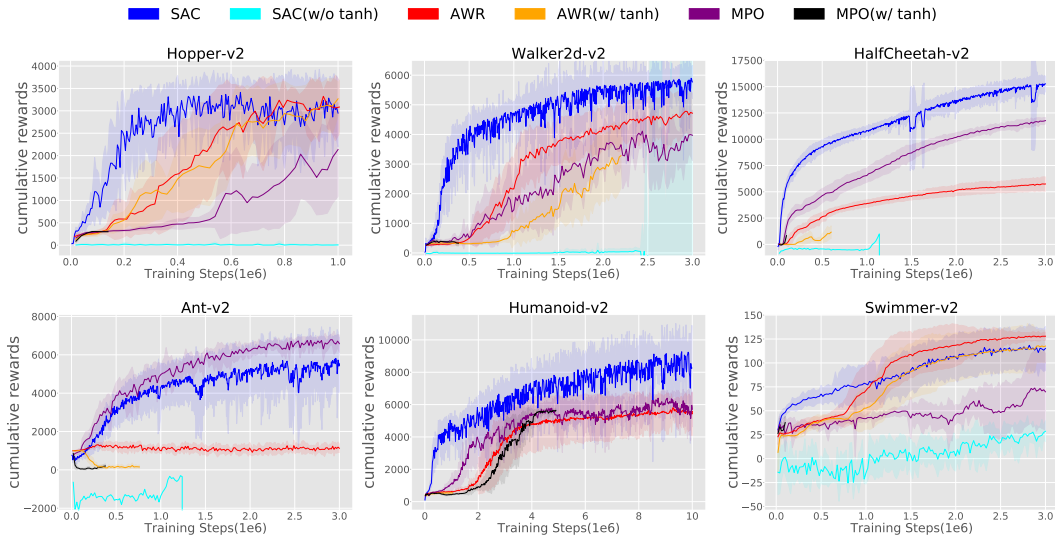


Figure 9: The learning curves of Table 15. We test SAC without tanh-squashed distribution, AWR with tanh, and MPO with tanh. SAC without tanh transform (using MPO action penalty instead) results in drastic degradation of the performance, which can be caused by the maximum entropy objective that encourages the maximization of the covariance. AWR and MPO with tanh squashing become numerically unstable. A line that stopped in the middle means that its training has stopped at that step due to numerical error.

## H.2 Network Architecture: Whole Swapping

In contrast to prior works on TRPO and PPO, the network architecture that works well in all the off-policy inference-based methods is not obvious, and the RL community doesn't have an agreeable default choice. Since the solution space is too broad without any prior knowledge, one possible ablation is that we test 3 different architectures that work well on at least one algorithm.

To validate the dependency of the performance on the network architecture, we exchange the configuration of the policy and value networks, namely, the size and number of hidden layers, the type of activation function, network optimizer and learning rate, weight-initialization, and the normalization of input state (See Appendix A). All other components remain the original implementations.

However, this ablation study might end up the insufficient coverage and the unclear insights. We broke down the network architecture comparison into the one-by-one ablations of activation and normalization, and experimented with finer network sizes.

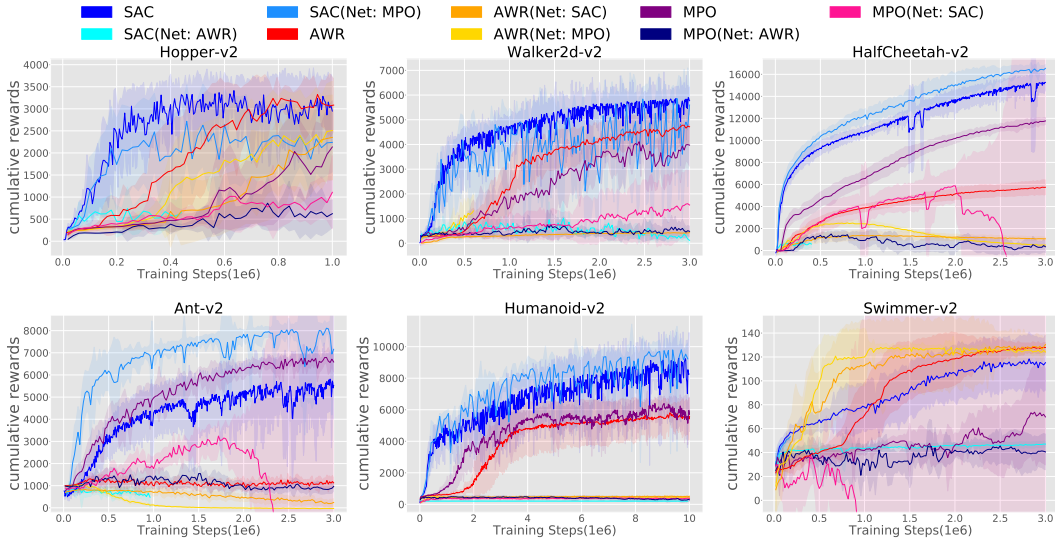


Figure 10: Swapping network architectures between each methods. These results suggest that these off-policy inference-based algorithms might be fragile with other network architectures and more co-dependent with architectures than on-policy algorithms. A line that stops in the middle means that training has stopped at that step with numerical error due to NaN outputs.

Algorithm	Architecture		
	MPO	AWR	SAC
MPO	2136 ± 1047	623 ± 316	1108 ± 828
AWR	2509 ± 1117	<b>3085 ± 593</b>	2352 ± 960
SAC	2239 ± 669	651 ± 381 <sup>†</sup>	3013 ± 602

Table 16: Results in Hopper-v2 environment (<sup>†</sup>numerical error happens during training). All results are averaged over 10 seeds and we also show their standard deviations.

Algorithm	Architecture		
	MPO	AWR	SAC
MPO	3972 ± 849	481 ± 210	1548 ± 1390
AWR	1312 ± 680 <sup>†</sup>	4717 ± 678	428 ± 89
SAC	5598 ± 795	117 ± 164	<b>5820 ± 556</b>

Table 17: Results in Walker2d-v2 environment (<sup>†</sup>numerical error happens during training). All results are averaged over 10 seeds and we also show their standard deviations.

Algorithm	Architecture		
	MPO	AWR	SAC
MPO	11769 ± 321	339 ± 517	−∞
AWR	485 ± 57	5742 ± 667	1060 ± 146
SAC	<b>16541 ± 341</b>	589 ± 367 <sup>†</sup>	15254 ± 751

Table 18: Results in HalfCheetah-v2 environment (<sup>†</sup>numerical error happens during training). All results are averaged over 10 seeds and we also show their standard deviations.

Algorithm	Architecture		
	MPO	AWR	SAC
MPO	6584 ± 455	967 ± 202	−∞
AWR	−30 ± 12	1127 ± 224	243 ± 167
SAC	<b>7159 ± 1577</b>	479 ± 463 <sup>†</sup>	5532 ± 1266

Table 19: Results in Ant-v2 environment (<sup>†</sup>numerical error happens during training). All results are averaged over 10 seeds and we also show their standard deviations.

Algorithm	Architecture		
	MPO	AWR	SAC
MPO	5709 ± 1081	288 ± 126	371 ± 72
AWR	420 ± 30	5573 ± 1020	507 ± 48
SAC	<b>9225 ± 1010</b>	205 ± 0	8081 ± 1149

Table 20: Results in Humanoid-v2 environment. All results are averaged over 10 seeds and we also show their standard deviations.

Algorithm	Architecture		
	MPO	AWR	SAC
MPO	70 ± 40	41 ± 15	−∞
AWR	124 ± 3	128 ± 4	<b>130 ± 8</b>
SAC	53 ± 6 <sup>†</sup>	47 ± 3	114 ± 21

Table 21: Results in Swimmer-v2 environment (<sup>†</sup>numerical error happens during training). All results are averaged over 10 seeds and we also show their standard deviations.